

ORIGINAL PAPER

Astri J. S. Kvassnes · Anita Hetland Strand
Heidi Moen-Eikeland · Rolf Birger Pedersen

The Lyngen Gabbro: the lower crust of an Ordovician Incipient Arc

Received: 26 January 2004 / Accepted: 10 August 2004 / Published online: 17 September 2004
© Springer-Verlag 2004

Abstract We present evidence for the origin of the Lyngen Gabbro of the Ordovician Lyngen Magmatic Complex in Troms, Northern Norway. The two magmatic suites of the Lyngen Gabbro strike parallel NNE-SSW, and have distinct magmatic signatures. We define these signatures by using major- and trace-element analyses together with selected major- and trace-element mineral analyses and $^{143}\text{Nd}/^{144}\text{Nd}$ -isotope whole-rock analyses of gabbroic to tonalitic plutonic rocks from seven detailed cross-sections from this large gabbro-complex. The Western suite of the Lyngen Gabbro precipitated from magma that may have been derived from the same system as the associated volcanic rocks. The gabbros have high An-content ($\text{An}_{>90}$) of their plagioclases relative to co-existing mafic minerals. Together with somewhat high $\epsilon_{\text{Nd}(t)}$ values (+6), this implies that the parental magmas were hydrous tholeiites similar to those found in back arc basins today. The Eastern suite, on the other hand, consist of cumulates that were precipitated from melts resembling those of ultra-depleted high-Ca boninitic magmas found in fore-arcs. Extremely high-An plagioclases ($\text{An}_{>95}$) co-exist with evolved mafic minerals and oxides, and the $\epsilon_{\text{Nd}(t)}$ values are lower (+4) than in the Western suite. The Eastern suite has no volcanic counterpart, but dikes intersecting the suites have compositions that possibly represent its parental magma. The oceanic Rypdalen Shear Zone generally separates the two suites in the

north, but several non-tectonic transitions from boninitic to tholeiitic signatures southwards advocate that the magmatism happened concurrently. The magmatic proximity between the suites, the hydrous magmatism and the absence of a silicic or calc-alkaline mature arc section, suggests that the Lyngen Gabbro formed in the Iapetus Ocean under conditions presently found in incipient arcs later emplaced as outer arc highs.

Introduction

The lower mid-ocean crust is generally inaccessible, and its origin and nature have therefore often been studied in ophiolites. In turn, ophiolites are often used to determine the size and type of ocean-basin that closed to form a given mountain range. However, many authors have inferred that most ophiolites are the remnants of mid-ocean crust (Nicolas 1989; Elthon et al. 1994), whereas other authors have suggested that many ophiolites formed in ocean arc settings (e.g. Miyashiro 1973). In order to deduce the tectonic events during an orogeny, the environmental ambiguity that ophiolites may represent must be resolved using geochemical and petrologic techniques.

The mid-ocean ridges are dominated by near-dry magmas erupting along a single, narrow, volcanic zone. Arcs, on the other hand have hydrous magmas erupting expansively along the trench. For example, transects through the Izu-Bonin arc in the Southwest Pacific comprises, from east to west, an outer arc high and fore-arc, a small intra-oceanic arc, and an actively spreading back-arc basin (Crawford et al. 1981). The back-arc basin have magma sources similar to those from mid-ocean ridges although melted with the aid of plate-derived water, the arc magmatism is strongly influenced by slab-derived material and melting in the mantle-wedge, and the fore-arc comprise the extremely depleted boninitic-type magmatism. The outer-arc high represent the

Editorial Responsibility: T. L. Grove

A. J. S. Kvassnes (✉)
Woods Hole Oceanographic Institution, IFM-GEOMAR,
Kiel, Germany
E-mail: akvassnes@ifm-geomar.deA. H. Strand
Statoil, 4035 Stavanger, NorwayH. Moen-Eikeland
Nipefjellet 83, 5300 Klepppestø, NorwayR. B. Pedersen
Department of Earth-Science, University of Bergen, Allegt 41,
5007 Bergen, Norway

incipient arc made up of interspersed boninitic and tholeiitic magmatism.

The extensive in-situ and experimental research into the petrologic and geochemical evolution of the crust and mantle in mid-ocean and supra-subduction zone environments give us valuable tools to understand and classify the origin of ophiolites. Isotope geochemistry and trace-element geochemistry have been used to support the theory that materials derived from the down-going plate are introduced into the subduction-zone mantle wedge that subsequently melt. In addition, assimilation of existing mantle rocks and crustal material may be assimilated into the ascending magma (e.g. AFC, DePaolo 1981). During crystal fractionation after emplacement, the concentration of water in a melt affects both the mineral reaction-series (Gaetani et al. 1993) and the composition of the solid-solution minerals that precipitate (Housh and Luhr 1991; Arculus and Wills 1990).

In this study, we used such petrologic and geochemical techniques to determine the origin of the Ordovician Lyngen Magmatic Complex. We show that the Lyngen Gabbro represents the lower crustal transition from MAR-like hydrous magmatism to high-Ca boninitic magma of a much more depleted source, conditions similar to like those in incipient arc environments.

Geological setting

The Norwegian Caledonides represent a stack of thin nappes thrust eastwards onto the Baltoscandian platform in late Silurian/early Devonian time (Dallmeyer and Andresen 1992). The Uppermost Allocthon is derived from spreading-ridges, rifted island arcs and marginal basins that existed within the consumed Iapetus Ocean (Andresen and Stelthenpohl 1994). The Lyngen Magmatic Complex is one of these Lower-Ordovician age ophiolite-complexes, with MOR-, IAT-, boninitic-, calc-alkaline- and alkaline affinities (Dunning and Pedersen 1988) indicating the association with island arc development (Pedersen and Furnes 1991).

The Lyngen Magmatic Complex

The Lyngen Magmatic Complex dominates the Lyngen Peninsula and contains the largest massif of gabbroic rocks known in the Scandinavian Caledonides (Fig. 1) (Munday 1974). It has been postulated to be a dismembered ophiolite complex (Minsaas and Sturt 1985), as no mantle section or sheeted-dike complex has been identified. The Lyngen Magmatic Complex comprises the Lyngen Gabbro, the Aksla Volcanics, and the Kjosens Greenschist (Furnes and Pedersen 1995). Its minimum age is Llanvirnian-Arenigian (469 ± 5 Ma) (Oliver and Krogh 1995), as determined from a tonalite intrusion in the southern part of the Kjosens Greenschist. The complex has undergone Caledonian deformation, and

large low-angle thrust faults dipping to the west intersect the complex. Hence, there may be some repetition of units due to tectonic events.

The Lyngen Gabbro is, by far, the dominant component of the Lyngen Magmatic Complex. A gravity profile has shown that the Lyngen Gabbro is wedge-shaped with the maximum thickness in the west (Chroston 1972). The Lyngen Magmatic Complex has been subdivided into a Western and Eastern suite, both trending NNE-SSW, based on different petrological and geochemical characteristics (Furnes and Pedersen 1995). The Lyngen Gabbro contains large shear zones, originally named Rypdalen Shear Zone, that separate the Western and Eastern suites in places and are accompanied by numerous variably sized dunitic and wehrlite bodies. Later dikes with a wide range of compositions intersect the Lyngen Gabbro and Rypdalen Shear Zone, leading Slagstad (1995) to interpret the shear zones to be of oceanic origin. The ultramafic rocks and the cross-cutting dikes are not the subject of this geochemical study, and will only be described as a part of the general geology. Most of the rocks of the Lyngen Gabbro have been extensively uralitized and saussuritized (Randall 1971).

The Aksla Volcanics trend NNE-SSW along a narrow zone ~15 km long and 400 m wide, in the South-western part of the Lyngen Peninsula, near Lakselvbukt (Fig. 1). The rocks are mainly deformed greenschist-facies pillow-lavas, hyaloclastite breccias and dikes of mid-ocean ridge (MORB) to Island Arc Tholeiite (IAT) affinities (Furnes and Pedersen 1995). An imbricated slab of gabbro, up to 600 m wide, has a sheared, sub-vertical contact to the overlying sedimentary rocks in the Balsfjord Group (Minsaas and Sturt 1985; Kvassnes 1997). The gabbro is varitextured and cut by numerous basic dikes, assumed associated with the Aksla Volcanics. The Eastern, sub-vertical contact between the Aksla Volcanics and the layered and high-level gabbros of the Lyngen Gabbro trend N-S, and is strongly sheared.

The Kjosens Greenschist outcrops from Strupen and southward, defining the easternmost part of the Lyngen Magmatic Complex. It comprises pillow lavas, volcanics and undifferentiated greenschists of MORB to island-arc tholeiite (IAT) affinities (Furnes and Pedersen 1995). The rocks of the Kjosens Greenschist are strongly sheared and deformed.

The gabbroic rocks and associated layered series from seven profiles throughout the Lyngen Gabbro have been sampled for this study. Only one traverse was sampled in each area. The areas north of the Kjosens Fjord are the Iddu area in the far north (70 samples, including a detailed profile of 12 samples), Strupen in the east (128 samples), and Skaidevarri in the central part (91 samples). Isskardet is in the west, south of the Kjosens Fjord (23 samples), Ellendalen lies east of the contact with the volcanic rocks (18 samples), Goverdalen is the valley to the northeast of Ellendalen (37 samples), and Veidalen is the valley in the central south (40 samples). The Norwegian Chart Service maps

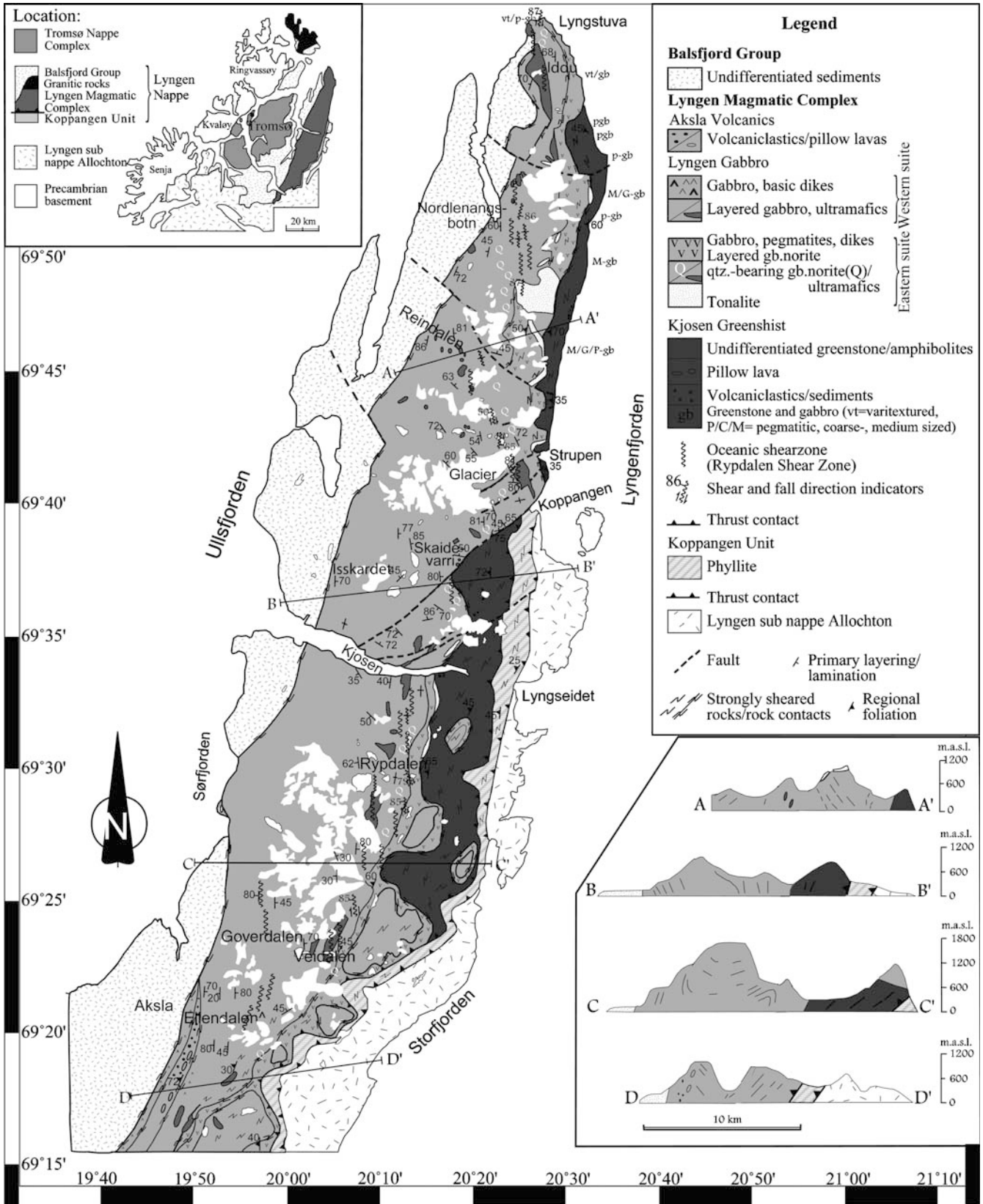


Fig. 1 The general geology of the Lyngen Peninsula (modified from Slagstad 1995). The seven profile names are listed on the figure. Iddu, in the north, Strupen in the east, Skaidevarri north of the Kjosen Fjord, Isskardet Northwest of Kjosen, Ellendalen in the far Southwest, Goverdalen to the northeast of the latter and Veidalen in the southeastern part of the Western suite. Four cross-sections are also shown, indicating the steep layering and folding in the Lyngen Gabbro. The peninsula is about 100 km from North to South

1634IV, 1634 V, 1633IV and 1533I in the series M711 cover the area.

The Eastern suite of the Lyngen Gabbro

Iddu

Iddu, on Lyngstuva, is the northernmost mountain of the Lyngen peninsula. The sample area is less than 1 km² and comprises gabbroic rocks and tonalites cut by basaltic dikes. Amphibolite-grade shear-zones crosscut the gabbros (Slagstad 1995), and basaltic dikes that have similar geochemical signatures as the host gabbros cut the shear-zones. Thus, these shear-zones have been interpreted to be of oceanic origin. In addition, later, possibly Caledonian, high-angle normal faults crosscut the section.

The tonalites have been classified into two groups: shearzone-related tonalites or layered tonalites (Moen-Eikeland 1999). The layered tonalites, interpreted to be the felsic fractionates of the original magma, are characterized by large gray-black, lens-shaped, quartz-grain aggregates in a groundmass of quartz, plagioclase, and pyroxene. The augen can be up to 1.5 cm in size and their orientation follows the layering. The shearzone-related tonalites, interpreted by Selbekk (1995) to be the result of anatectic melting of amphibolized gabbro, are fine-grained and consists of plagioclase, quartz, pyroxene and amphibole (Selbekk et al. 1998, 2002). As those tonalites are regarded as a later crosscutting feature, they are not included in our dataset.

The gabbroic rocks are subdivided into massive and laminated gabbro, varitextured leucogabbro and gabbroic pegmatites (Moen-Eikeland 1999). Massive and pegmatitic gabbros occur together. The massive gabbro is fine-grained with plagioclase, two pyroxenes, primary amphibole, and magnetite. Coarser patches often show larger grains of magnetite. The gabbroic pegmatites have plagioclase, pyroxenes, amphibole, magnetite, and quartz and the grain-sizes vary from 1 to 15 cm. The laminated gabbros are composed of plagioclase, pyroxenes, amphibole, and some quartz.

Strupen

The sampled area consists mainly of layered plagioclase-bearing rocks that can contain quartz as a euhedral mineral. Five major lithologies have been described (Hetland 1996). Stratified layers (Type 1) grade from

leuco- to melagabbro, exhibiting plagioclase lamination, small subhedral clinopyroxene crystals, and 5–10 cm-long clinopyroxene-augen oriented parallel to the layering. The oxide-rich gabbroic layers (Type 2) with plagioclase-rich zones have sharp contacts with the adjacent layers. Stratified, oxide-rich gabbroic layers (Type 3) have increasing amounts of oxide upwards. Oxide and quartz-bearing “gabbroic” layers (Type 4) comprise distinctive lamination defined by quartz grains oriented parallel to the layering. The quartz-rich “gabbroic” rocks of this lithology have up to 50% quartz and are unique and characteristic features of the Eastern suite, although the volume of these rocks does not exceed 5% in the section. Tonalites (Type 5) is found as to 5–6 m thick layers. The latter rock type often occurs above the oxide-rich layers, and tends to interfinger with them with flame- and load-cast structures. The profile sampled is 95 m long, and has been sampled perpendicular to the layering.

The Western suite of the Lyngen Gabbro

Isskardet

The area consists of gabbro showing pronounced compositional layering that is steeply dipping and strikes N–S and perpendicular to the valley. The modal layering is typically of 5–10 m scale with smaller scale (10–50 cm) layering locally superimposed. The thicker layers can be traced laterally for 1–2 km across the valley. The rocks are generally medium to fine-grained with granulitic mineral-textures suggesting deformation at a late-magmatic stage. They range from olivine-gabbros to oxide-gabbronorites, and no tonalites have been sampled.

Ellendalen

An imbricated gabbro-slab west of the Aksla Volcanics is composed of high-level varitextured and massive gabbros cut by mafic dikes. The dikes trend N–S, with a 60° and 80° dip to the west. Lakselvdalstindane, the northern wall of Ellendalen is dominated by layered gabbros folded in a large drag-synform with an N–S trending fold-axis dipping 40° to the north (Randall 1971). The layering can be followed for at least 2,200 m along the mountain scarp and crops out from 300 to 1,400 m above sea level (Kvassnes 1997). The sequence in this mountain may therefore represent 850 m of layered gabbro. At the innermost part of Ellendalen, an up to 1 km wide, sub-vertical, N–S trending anastomosing shear zone caused a large antiformal drag-fold to form in the layered gabbros. Isotropic and varitextured gabbros have been found in the lower part of these mountain-scarps, where sampling ended. The gabbroic rocks have, in general, undergone extensive greenschist alteration, and magmatic minerals are not preserved except for rare cores of clinopyroxene.

Table 1 Representative whole-rock analyses of the Western suite of the Lyngen Gabbro

Location	Isskardet	Isskardet	Isskardet	Ellendalen	Ellendalen	Ellendalen	Ellendalen	Goverdalen	Goverdalen	Goverdalen	Goverdalen
Sample no.	LYIS-2	LYIS-16	LYIS-26	92LY119	94LY23	94LY25	94LY29	95LY5	95LY34	95LY38	95LY39
Description				Metagb	Gabbro	Varitex gb	Gabbro	Microgb	Melagb	Gabbro	Melagb
Place in profile				9,350	7,150	7,000	5,400	4,550	2,535	2,280	2,215
W ≤ E											
Major elements (XRF)											
SiO ₂	47.5	43.2	44.3	51.3	42.4	36.2	38.2	39.6	43.2	48.8	45.6
TiO ₂	0.23	0.83	0.75	0.50	0.03	2.88	1.81	2.14	1.49	1.57	0.13
Al ₂ O ₃	17.7	18.1	19.2	15.1	3.8	8.2	16.1	13.6	11.4	15.0	16.2
Fe ₂ O ₃ *	7.7	13.7	12.0	10.1	13.0	27.7	20.8	21.2	22.9	16.0	6.9
MnO	0.16	0.16	0.15	0.19	0.19	0.24	0.18	0.21	0.22	0.22	0.12
MgO	9.3	9.2	8.2	7.9	28.2	9.2	5.3	7.3	8.6	6.1	12.2
CaO	16.1	13.8	14.7	11.2	9.7	11.4	12.7	12.8	12.4	10.0	16.3
Na ₂ O	0.79	0.70	0.84	2.78	0.00	1.44	0.68	0.43	0.76	2.87	0.69
K ₂ O	0	0	0	0.16	0.00	0.03	0.02	0.00	0.00	0.01	0.00
P ₂ O ₅	0.01	0.00	0.02	0.08	0.01	0.02	0.01	0.01	0.00	0.10	0.01
LOI	1.4	0.8	0.1	2.1	1.5	1.8	2.6	2.6	0.9	0.4	1.4
Sum	100.8	100.5	100.2	101.3	98.6	98.7	98.4	99.9	101.8	100.9	99.5
Trace elements (XRF)											
V	194	787	705	191	648	600	1,182	895	1,134	452	106
Cr	47	105	67	29	33	49	63	40	77	28	216
Co	43	61	49	43	47	68	64	73	71	47	49
Ni	35	48	17	37	11	25	77	32	77	15	101
Cu	16	13	14	41	25	120	229	147	242	64	178
Zn	36	41	38	58	83	118	88	99	60	81	33
Rb	1	2	0	1	0	0	0	0	0	0	0
Sr	170	146	166	198	435	64	164	133	97	178	107
Y	7	6	5	25	6	17	8	9	11	23	6
Zr	13	13	13	39	15	18	9	11	11	22	7
Nb	2	2	2	5	2	3	4	6	7	6	4
Ba				86	71	0	74	55	47	109	36
La	0	0	0	5	0	0	13	0	0	5	0
S					0.07		0.26	0.29	0.79	0.20	0.24
Ce	14	12	15	19	12	14	0	16	14	8	15
Nd	7	4	7	4	8	10	4	6		10	5
Mg#	70.5	57.4	57.7	60.9	81.2	39.8	33.7	40.7	42.9	43.0	77.9

Notes: Fe₂O₃* is all Fe measured as Fe₂O₃. Mg# is $100 \times \text{MgO} / (\text{MgO} + 0.899 \times \text{Fe}_2\text{O}_3^*)$

"Place in profile" indicates the relative distance east of the starting-point for each of the profiles. Strupen and Skaidevarri are individual profiles, Ellendalen, gb gabbro, tex textured, pegm pegmatite, ol olivine, ox magnetite and/or ilmenite, diss disseminated, troct troctolite, hbl hornblende, qz quartz, pyxite pyroxenite

Goverdalen

To the east of the same shearzone in Goverdalen, isotropic and varitextured gabbros outcrops, and gradually develop into a layered gabbroic section that can be followed eastwards through the valley and towards the Goverdalen Lake (Fig. 1) (Kvassnes 1997). The gabbroic rocks of the Southwestern part of Mt. Nállangaisi contain plagioclase-free wehrlite bodies close to the shear-zone. Layered gabbros are exposed on the steep walls of the valley, and the shear-zone outcrops on the valley floor, where anatectic tonalites are crosscut by inferred oceanic dikes. East of the shear-zone, layered and laminated gabbros were sampled towards the Goverdalen Lake. The rocks are generally gabbro-norites, olivine is mostly absent in the plagioclase-bearing rocks and only one, less than a metre wide, wehrlite layer is associated with the section. The most evolved gabbros are rich in magnetite and ilmenite. The rocks have undergone extensive greenschist alteration,

and epidiosites have been found in the west of this valley.

The transition between the suites

Skaidevarri

This 160-m transect is an east-west profile along the south side of Skaidevarri. The rocks range from troctolitic gabbros through olivine-gabbros, gabbros, olivine-gabbro-norites, olivine-oxide-gabbros and oxide-gabbros. The rocks are mostly uniform with some fine, near-vertical layering in places. Sampling was done perpendicular to the layering. Some of the gabbros have undergone greenschist-facies metamorphism, with saussuritized plagioclase, iddingsitized olivine, and clinopyroxene partly altered to green amphiboles with only small amounts of relict magmatic cores. The alteration ranges from 10 to 100%. The fresh rocks show poikilitic

Veidalen 95LY127 Gabbro 2,080	Veidalen 95LY123 Melagabbro 1,900	Veidalen 95LY106 Gabbro 1,560	Veidalen 95LY94 Gabbro 1,468	Veidalen 95LY87 Gabbro 1,429	Veidalen 95LY58 Metagb 550	Skaidevarri 90LY141 Olgbnorite 10.5	Skaidevarri 90LY158 Olgbnorite 36.5	Skaidevarri 90LY168 Olivinegb 51.5	Skaidevarri 90LY190 Gabbro 93	Skaidevarri 90LY192 Oxgbnorite 96	Skaidevarri 90LY218 Troct gb 149	Skaidevarri 90LY224 Oxgb 160.5
46.40	39.81	48.79	46.15	50.43	40.66	46.72	49.18	45.49	46.9	44.1	46.49	43.87
0.1	1.16	0.1	0.09	0.05	0.04	0.17	0.26	0.16	0.38	0.96	0.15	0.69
16.13	11.9	10.74	14.65	4.81	22.79	18.74	11.16	16.45	13.79	14.84	21.12	18.69
7.75	22.7	6.79	7.96	5.92	7.33	7.19	9.58	9.74	9.95	14.72	7.96	11.17
0.13	0.17	0.14	0.16	0.11	0.11	0.12	0.19	0.15	0.15	0.16	0.14	0.14
11.26	8.44	14.32	12.24	20.73	9.45	9.65	13.09	12.04	10.29	9.59	8.68	7.31
15.24	12.79	18.79	17.38	18.04	15.91	15.4	15.52	14.04	15.84	14.56	15.12	15.49
0.56	0.57	0.15	0.39	0.12	0.57	0.82	0.42	0.49	0.63	0.67	0.86	1.07
0.02	0.11	0	0.01	0.01	0.09	0	0	0	0.02	0.02	0	0.03
0.01	0.02	0.02	0.02	0	0	0	0	0.01	0.01	0	0.02	0.01
2.34	2.25	0.42	1.72	0.627	3.05	1.78	1.11	2.14	1.9	1.15	0.46	2.13
99.95	99.9	100.24	100.77	100.85	100	100.6	100.5	100.7	99.87	100.79	101	100.59
101	976	146	140	111	68	105	193	94	300	659	71	529
185	46	890	350	2496	260	207	607	98	311	150	63	76
52	78	51	57	52	47	45	55	58	62	65	47	56
73	12	57	80	260	57	84	83	85	67	67	36	39
135	66	49	229	12	9	118	103	112	205	187	14	152
33	78	18	41	20	36	22	35	32	32	29	26	29
0	0	0	3	0	6	2	2	0	4	3	0	3
119	87	45	91	13	133	148	76	131	111	107	169	151
3	11	0	3	0	0	6	9	6	11	8	7	8
8	9	6	6	5	7	11	9	9	10	9	11	9
4	4	4	5	4	4	0	4	0	1	1	0	2
53	72	35	40	27	46	32	93	73	109	125	17	50
0	0	0	5	6	0							
0.19	0.03	0.03	0.08	0.03	0.02							
12	7	13	16	18	10	18	19	8	20	24	15	7
10	6	6	6	5	5							
74.3	42.6	80.8	75.4	87.5	72.0	72.81	73.16	71.15	67.35	56.51	68.51	56.62

Goverdalen and Veidalen has a common profile
ton tonalite

pink clinopyroxene, brown hornblende and plagioclase; the latter occurs as euhedral chadacrysts in clinopyroxene or has been deformed during high-temperature deformation to microcrystalline aggregates. Each of the magmatic mineral-types has inclusions of the other types in them.

Veidalen

East of the Goverdalen-lake, a very complicated layered sequence of wehrlites and gabbros crop out (Kvassnes 1997). The layering appears to be deformed at a late magmatic stage, with multiple ductile folds, dunite pods and flame-structures. The gabbros are fine grained, and plagioclase is so dark that the rocks appear to be pyroxenites in outcrop. Some of the gabbros have high-Ca garnets and blue amphibole. The sequence looks similar to the Middle Series of the Rum Layered Suite on the Western coast of Scotland as described by Emeleus et al. (1996).

Mt. Balggesvarri, to the north of this valley, is dominated by layered gabbros, and the anastomosing shear-zone causes the layering to be folded into a synformal dragfold. At the foot of the mountain, a large low-angle, westward dipping thrustfault intersects the gabbro and an ultramafic body crops out at the top. Entering Veidalen, an approximately 2 km thick sequence of laminated metagabbro cut by basic and intermediate dikes can be followed towards another large oceanic shear-zone. Within the shear-zone, a large ultramafic body of wehrlite and dunite (2 km long and 0.5 km wide) crops out from Sydbreen in the north to Veidalsvatnet in the south. A smaller body of dunite is also seen below the small glacier in Nállancohka south of Veidalsvatnet.

From the middle of Veidalsvatnet and eastwards into Veidalen and Gaskacóhka, quartz-bearing gabbros and quartz-rich tonalites typical of the Eastern suite of the Lyngen Gabbro appear. There are no geochemical data from this part of the section. the Kjosens greenschist crops out on the eastern side of Mt. Njállavarre.

Table 2 Representative analyses from the Eastern suite of the Lyngen Gabbro

Location Sample no.	Skaidevarri 90-LY-134	Skaidevarri 90-LY-137	Skaidevarri 90-LY-140	Iddu HLY-9-93	Iddu HLY-10-93	Iddu HLY -41-93	Iddu HLY2.3 -4PA	Iddu HLY -4PA	Iddu ton.-qz-gran.	Lith. 1	Lith. 2	Lith. 3	Strupen Lan-58	Strupen Lan-72	Strupen Lan-93	Strupen Lan-96
Description	Gbnorite	Gabbro	Olgabbro	qz-gabbro	ton.-qz-gran.	Melagb qz-gabbro	Melagb qz-gabbro	ton.-qz-gran.	Lith. 1	Lith. 2	Lith. 3	Lith. 4	Strupen Lan-58	Strupen Lan-72	Strupen Lan-93	Strupen Lan-96
Place in profile W ≤ E	0	4.5	9						19.75	26.1	34.75	43.25	Lith. 5	Lith. 5	Lith. 5	Lith. (ox gb)
Major elements																
(XRF)	47.3	46.7	47.3	45.8	61.3	41.3	56.0	52.2	74.4	49.1	46.6	46.2	60.8	43.7	75.9	
SiO ₂	0.13	0.11	0.10	0.67	0.12	0.61	0.33	0.19	0.18	0.13	0.17	0.22	0.40	0.38	0.03	
TiO ₂	15.4	17.8	14.8	14.0	11.5	20.1	14.4	8.5	13.8	8.4	18.0	19.1	14.9	17.0	13.0	
Al ₂ O ₃	6.2	5.3	5.7	18.3	9.9	15.7	9.3	15.0	3.6	8.1	11.8	12.9	9.6	16.6	0.9	
Fe ₂ O ₃ *	0.11	0.10	0.10	0.34	0.19	0.24	0.18	0.33	0.06	0.17	0.20	0.22	0.13	0.19	0.02	
MnO	12.3	10.1	12.5	7.4	8.1	5.5	6.9	14.5	0.9	14.1	9.3	7.9	3.1	8.1	0.1	
MgO	17.0	17.9	17.8	11.1	7.9	14.0	8.8	8.7	4.9	17.5	13.9	13.6	9.4	14.1	6.4	
CaO	0.35	0.49	0.19	1.33	1.50	0.74	1.60	.80	2.54	0.05	0.26	0.39	0.21	0.37	1.08	
K ₂ O	0.03	0.02	0.00	0.14	0.00	0.04	0.75	0.00	0.05	0.01	0.00	0.00	0.00	0.00	0.01	
P ₂ O ₅	0.00	0.00	0.00	0.01	0.02	0.17	0.07	0.01	0.01	0.01	0.01	0.00	0.00	0.01	0.02	
LOI	2.5	2.6	2.5	1.4	0.6	3.2	1.2	0.4	0.7	1.0	0.0	0.2	0.1	1.9	1.1	
Sum	101.4	101.0	101.0	100.5	101.2	101.5	99.6	100.7	101.2	98.5	100.0	100.6	98.7	101.3	98.5	
Trace elements																
(XRF)	118	120	123	563	180	302	164	172	42	215	271	273	186	561	7	
V	534	660	849	31	499	29	518	1858	3	2035	15	22	6	37	6	
Cr	46	39	42	58	33	57	39	42	10	55	61	57	32	63	0	
Ni	143	82	141	10	92	8	99	194	7	129	33	21	6	27	5	
Cu	217	66	170	75	13	34	32	19	18	28	126	109	55	217	8	
Zn	17	11	8	141	90	101	76	147	34	41	64	70	51	65	2	
Rb	3	0	0	6	2	1	21	1	3	2	0	0	0	0	0	
Sr	87	115	74	109	119	229	230	63	194	36	97	103	100	90	122	
Y	6	5	4	15	12	10	16	24	8	2	2	2	2	1	3	
Zr	9	10	9	15	13	14	35	20	19	19	17	16	17	6	14	
Nb	0	0	0	2	1	3	5	4	2	2	5	4	4	4	3	
Ba	33	76	58	145	0	1	156	47	52	5	11	3	4	6	1	
La				10	4	10	14	10	8	18	20	8	23	13	7	
S	21	21	19	0.31	0.03	0.08	0.03	0.03	0.03	0.03	0.08	0.18	0.09	0.29	0.02	
Ce				32	0	15	28	8	0	2	57	41	31	32	27	
Nd				8	0	12	14	12	0	2	3	7	2	2	0	
Mg#	66.3	65.6	68.9	28.6	44.7	25.8	42.7	49.1	20.1	63.4	44.0	38.0	24.3	32.7	13.7	

Notes: Fe₂O₃* is all Fe measured as Fe₂O₃. Mg# is 100×MgO/(MgO+0.899×Fe₂O₃*)
 "Place in profile" indicates the relative distance east of the starting-point for each of the profiles. Strupen and Skaidevarri are individual profiles
 gb gabbro, ol olivine, qz quartz, ton tonalite, gran granite

Table 3 Representative isotope analyses of the Lyngen Gabbro

Sample	Sm (ppm)	Nd (ppm)	$^{147}\text{Sm}/^{144}\text{Nd}$	$^{143}\text{Nd}/^{144}\text{Nd}$	$^{143}\text{Nd}/^{144}\text{Nd}$ CHUR	Initial $^{143}\text{Nd}/^{144}\text{Nd}$	E_CHUR	$\epsilon_{(480\text{My})}$ CHUR
Skaidevarri								
90-LY-134	0.21	0.46	0.284	0.513055	0.51203	0.512162	7.962	2.60
90-LY-135	0.19	0.40	0.280	0.513117	0.51203	0.512236	9.162	4.05
90-LY-137	0.16	0.28	0.332	0.513374	0.51203	0.512330	14.178	5.89
90-LY-219	0.33	0.67	0.299	0.513303	0.51203	0.512364	12.792	6.55
Strupen								
Lan-1	0.12	0.21	0.363	0.513336	0.51203	0.512195	13.446	3.24
Lan-23	0.08	0.12	0.386	0.513337	0.51203	0.512125	13.467	1.88
Lan-58	0.07	0.14	0.326	0.513288	0.51203	0.512264	12.502	4.60
Lan-110	0.195	0.703	0.1680	0.512762	0.51203	0.512234	2.240	4.01
Isskardet								
LY-IS-9	0.11	0.32	0.211	0.513030	0.51203	0.512366	7.478	6.58
LY-IS-31	0.46	0.87	0.315	0.513365	0.51203	0.512374	14.007	6.75
Ellendalen								
92LY119	7.92	78.15	0.2289	0.513068	0.51203	0.512348	8.212	6.24
93LY20	0.95	7.42	0.2882	0.513208	0.51203	0.512302	10.943	5.34
94LY39	1.17	10.07	0.2625	0.513173	0.51203	0.512348	10.260	6.23
Goverdalen								
95LY2	0.53	4.24	0.2818	0.513187	0.51203	0.512301	10.534	5.32
95LY38	6.92	60.35	0.2589	0.513190	0.51203	0.512376	10.592	6.79
Veidalen								
95LY127	0.80	5.72	0.3156	0.513298	0.51203	0.512306	12.699	5.41
95LY106	0.47	2.81	0.3775	0.513373	0.51203	0.512186	14.162	3.08
Iddu								
Hly 2.8	0.06	0.23	0.154	0.512193	0.51203	0.511709	-8.856	-6.24
Hly 26-94	0.45	1.53	0.178	0.512604	0.51203	0.512044	-0.839	0.31
Hly 5 PA	0.84	2.15	0.236	0.512967	0.51203	0.512225	6.242	3.84
Hly 7 PA	0.9	2.27	0.24	0.513005	0.51203	0.512250	6.983	4.33
Dikes Goverdalen								
95LY72	1.396	5.995	0.1408	0.512125	0.51203	0.511683	-10.176	-6.75
95LY71	0.314	0.566	0.3357	0.513290	0.51203	0.512235	12.544	4.02
Dikes, Iddu								
HLY 2993	2.23	8.8	0.153	0.512781	0.51203	0.512300	2.614	5.30
Hly 36-93	1.29	6.39	0.122	0.511862	0.51203	0.511478	-15.313	-10.74

In addition to data from each area, dikes crosscutting the gabbros in Goverdalen and at Iddu are included for comparison

Methods

Whole rock analyses

Major and trace element analyses were performed at the University of Bergen. Fist size samples were crushed in a jaw crusher, and 80–100 cm³ were crushed to powder in an electrical agate mortar. The glass bead technique of Padfield and Gray (1971) was used for the major elements analyses and pressed-powder pellets for the trace elements analyses, using international basalt standards with recommended or certified values from Govindaraju (1994) for calibration. The analyses were carried out on a Phillips PW 1440 X-Ray fluorescence spectrometer. Instrumental precision for the major and trace elements for the glass-bead and pressed powder pellets have been documented by repeated analyses of representative samples. The relative standard deviations are close to 100% for low concentrations of the elements Zr, Y, Nb and P₂O₅. Representative whole-rock analyses are presented in Tables 1 and 2, and the entire dataset is available from supplemental Tables 1 and 2.

Mass spectrometry analyses

Seventy-three samples have been measured for Sm and Nd-isotopes on a Finnegan MAT 262, 9-collector, fully automated mass spectrometer (MS) at the University of Bergen. All chemical processing was carried out in a clean-room environment with HEPA filtered air supply and positive pressure. The reagents were either purified in two-bottle Teflon stills or passed through ion-exchange columns. Samples were dissolved in a mixture of HF and HNO₃. REE were separated by specific extraction chromatography using the method described by Pin et al. (1994). Sm and Nd were subsequently separated using a low-pressure ion-exchange chromatographic set-up with HDEHP coated Teflon powder (Richard et al. 1976). Sm and Nd were loaded on a double filament and analyzed in multidynamic mode. Nd isotopic ratios were corrected for mass fractionation using a $^{146}\text{Nd}/^{144}\text{Nd}$ ratio of 0.7219. Sm and Nd concentrations were determined using a mixed $^{150}\text{Nd}/^{149}\text{Sm}$ spike. Repeated measurements of the JM Nd-standard yielded an average $^{143}\text{Nd}/^{144}\text{Nd}$ ratio of $0.511113 \pm 15 (2\sigma)$ ($n = 62$). The

Table 4 Representative major-element mineral analyses of the Lyngen Gabbro

Sample no.	Plagioclase	An%	1 σ	Augite	Mg#	1 σ	Opx	Mg#	Olivine	Fo
Skaidevarri										
90LY138-1	Core (7)	94.7	0.85	core (5)	85.1	0.63			(6)	78.7
90LY138-1	Rim to cpx (2)	95.7	3.82	Rim (5)	85.3	0.74				
90LY141-2	Core (5)	83.9	0.42	Core (5)	78.8	0.33	(6)	74.5		
90LY141-2	Rim (5)	83.8	0.64	Rim to plag (6)	79.2	1.08				
90LY143-2	Core (3)	88.6	1.38	Core (5)	78.4	1.81			(6)	70.6
90LY143-2	Rim to cpx (4)	88.9	0.66	Rim to plag (5)	80.2	0.49				
Skaidevarri maximum		95.7			86.4			81.1		78.7
Skaidevarri minimum		83.8			75.3			70.5		66.9
Iddu										
1pa		52.6	2.03					60.7		
7pa		74.4	2.28		71.2	1.89		62.4		
18pb		67.4	1.24		73.9	1.26		64.6		
Iddu maximum		75.0			76.7			66.1		
Iddu minimum		52.6			71.2			60.7		
Strupen										
Lan-2		97.1			76.1			68.6		
Lan-20		92.6			72.6			63.7		
Lan-31		98.2			76.3			68.3		
Lan-74		93.7			70.6			58.0		
Strupen maximum		98.2			82.0			74.5		
Strupen minimum		90.5			69.6			57.0		
Goverdalen										
95LY34		77.2			72.5			64.9		
95LY35		79.0			73.8			67.0		
95LY38		48.6			66.9			56.8		
95LY39		87.2			79.4			75.2		72.3
95LY40		87.6			83.6					
Goverdalen maximum		87.6			83.6			75.2		72.3
Goverdalen minimum		48.6			66.9			56.8		72.3
Veidalen										
95LY127		86.6			72.1			64.4		68.1
95LY106		95.7			83.2			78.4		75.9
95LY94		95.3			79.9			74.3		
Veidalen maximum		97.7			88.0			83.8		83.5
Veidalen minimum		86.6			72.1			64.4		68.1
Isskardet										
IS-2	Core (5)	83.8	0.69	core (5)	75.9	0.61			(6)	64.2
IS-2	Rim (5)	84.5	1.94	rim (5)	75.8	0.70				
IS-16	Core (5)	84.2	0.96	core (5)	76.3	1.02	(6)	72.7	(6)	67.8
IS-16	Rim (5)	83.5	1.45	rim (5)	76.3	0.42				
IS-26	Core (5)	80.8	1.65	core (5)	75.2	0.43			(6)	67.1
IS-26	Rim (5)	82.2	2.55	rim (5)	75.3	0.20				
Isskardet maximum		84.5			76.4			72.7		67.8
Isskardet minimum		75.7			75.2			71.2		64.2

Notes: Where the information was available, the position of the analyses and the number of points () are listed. The minerals are listed so cores are aligned with cores, rims with rims. Orthopyroxene and olivine do not show any significant chemical zoning. All areas are represented, except for Ellendalen.

pl plagioclase, c core, r rim, cpx augite, opx orthopyroxene, Fo forsterite % of olivine

typical Nd blank level in the laboratory is 5 pg. Representative analyses are listed in Table 3, and the entire dataset is available from Supplemental Table 3.

Mineral analyses

Major element analyses of clinopyroxene, orthopyroxene, plagioclase, and olivine have been performed using an ARL-SEM-Q electron microprobe at the Nordic Volcanological Institute, Iceland. The microprobe analyses reported here are representative single-point analyses, unless so noted. All analyses were done with focussed beam (2 μm in diameter). The analyses were performed

with a beam potential of 15 kV, sample current of ~ 15 nA, 40 s counting times for peak, and mean atomic number (MAN) corrections for background. Standards used were basaltic glasses. Electron microprobe analyses of clinopyroxene, orthopyroxene, plagioclase, olivine and ore-minerals of 79 additional samples were carried out at the University of Bergen. These were done as standardless EDS-analyses on a scanning electron microscope (JEOL scanning microscope, JSM-6400), using the Tracor Northern energy dispersive analysing system (TN 5600), with a 20 kV beam. A final set of mineral analyses was made on an ARL-SEM-Q electron microprobe at the University of Bergen. All analyses were done with a defocussed beam (10 μm in diameter).

Table 5 Trace-element and rare-earth element mineral chemistry for ten samples from the Lyngen Gabbro

Sample	La (ppm)	Ce (ppm)	Nd (ppm)	Sm (ppm)	Eu (ppm)	Dy (ppm)	Er (ppm)	Yb (ppm)	Ti (ppm)	V (ppm)	Cr (ppm)	Sr (ppm)	Y (ppm)	Zr (ppm)
Goverdalen														
LY-95-39-cpx-c	0.12	0.62	1.25	0.86	0.41	1.67	0.89	0.99	1486	260	449	8.7	8.7	3.7
LY-95-39-cpx-r	0.14	0.67	1.03	0.68	0.34	1.51	0.84	0.87	1537	262	541	7.8	8.9	4.7
LY-95-34-cpx-c	0.23	1.29	2.76	1.85	0.59	3.75	2.14	2.34	2508	437	85	10.0	22.6	11.3
LY-95-34-cpx-r	0.24	1.17	2.28	1.50	0.60	3.65	2.11	2.12	2338	413	83	9.3	23.5	12.0
LY-95-38-cpx-c	0.54	3.53	9.32	5.76	1.52	12.18	6.64	7.04	2352	265	70	11.6	67.5	67.3
LY-95-38-cpx-r	0.60	4.21	9.75	6.20	1.52	12.62	6.82	7.72	2221	258	72	11.2	74.2	64.2
Veitdalen														
LY-95-87-cpx-c	0.02	0.11	0.24	0.18	0.06	0.25	0.22	0.21	339	236	1994	8.6	1.4	0.6
LY-95-87-cpx-r	0.01	0.08	0.26	0.14	0.06	0.20	0.14	0.17	371	255	1924	6.1	1.6	0.8
LY-95-96-cpx-c	0.04	0.21	0.40	0.35	0.16	0.52	0.30	0.31	872	299	1036	8.1	4.1	1.2
LY-95-96-cpx-r	0.12	0.62	0.96	0.63	0.36	1.36	1.05	0.83	2244	401	965	28.5	15.2	2.8
LY-95-127-cpx-c	0.32	1.65	2.86	1.69	0.51	3.41	1.99	1.98	3219	441	160	9.5	22.4	11.4
LY-95-127-cpx-r	0.39	1.66	2.81	1.71	0.51	3.50	1.85	2.04	2343	357	151	9.8	20.7	10.5
Strupen														
Lan38 cpx-c	0.06	0.34	0.49	0.26	0.12	0.54	0.32	0.32	869	310	2437	6.5	3.5	1.9
Lan38 cpx-r	0.07	0.30	0.40	0.25	0.13	0.50	0.37	0.37	857	312	2486	6.7	3.5	1.7
Lan47 cpx-c	0.05	0.29	0.48	0.30	0.20	0.95	0.63	0.76	1411	380	88	6.5	6.4	1.4
Lan47 cpx-r	0.03	0.25	0.41	0.28	0.16	0.84	0.49	0.60	723	248	90	5.5	3.3	1.3
Lan58 cpx-c	0.03	0.35	0.67	0.48	0.27	1.44	1.04	0.95	1158	280	88	6.0	7.2	2.2
Lan58 cpx-r	0.04	0.34	0.57	0.51	0.21	1.21	0.81	0.84	1067	283	89	6.6	6.1	2.0
Lan72 cpx-c	0.05	0.29	0.61	0.55	0.37	1.55	1.07	1.16	1675	202	80	8.6	11.2	2.0
Lan72 cpx-r	0.03	0.27	0.78	0.55	0.34	1.57	1.11	1.15	2779	198	80	8.1	10.8	1.8

All the analyses are listed as ppm

Cpx augite, *c* core, *r* rim. The errors are less than 10% for the REE, and less than 5% for the other trace elements

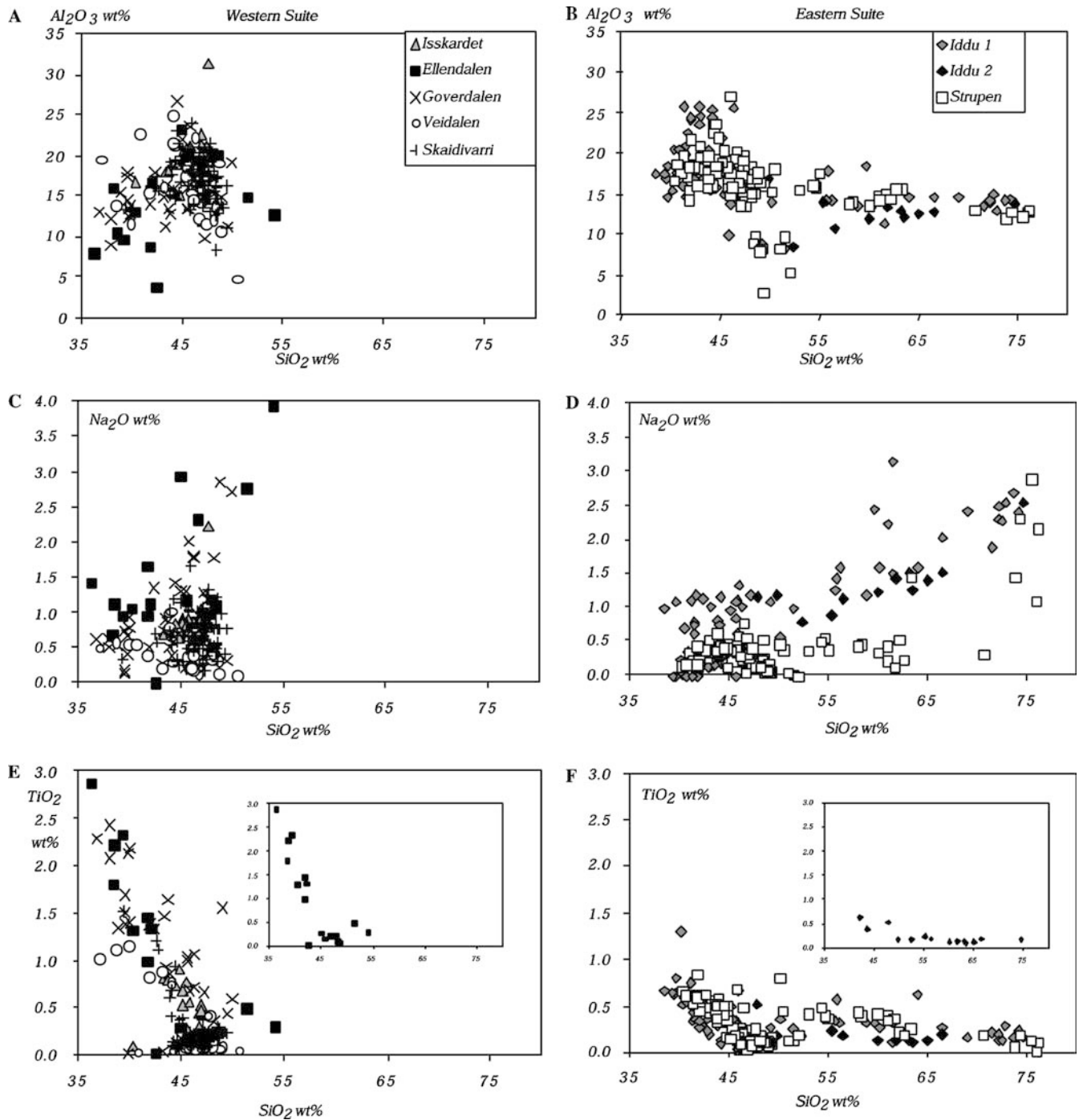


Fig. 2 Major element compositions of gabbroic whole-rocks sampled from seven different areas in the Lyngen Gabbro. **a**, **c**, and **e** show Harker diagrams for the Western suite, and **b**, **d**, and **f** the Eastern suite, respectively. Iddu has been separated into Iddu-1, the general sampling of the area, and Iddu-2, a detailed transition. The inserts in **e** (Ellendalen) and **f** (Iddu 2) show the difference between the two suites

The analyses were performed with a beam potential of 15 kV, sample current of 10 nA, 40 s counting times for peak and 10 s for background (MAN background correction for Si, Ca, Al and Fe). Standards used were basaltic glasses, minerals, and metals. Representative

analyses are listed in Table 4, and the entire dataset is available in Supplemental Table 4.

Ion-probe analyses

Three samples were selected from Goverdalen and Veidalen, representing the geochemical spectrum of plagioclase-bearing rocks in the areas. Four samples were selected from Strupen, representing four of the rock types spread out in the lower half of the profile. Unaltered cores and rims of clinopyroxene from these

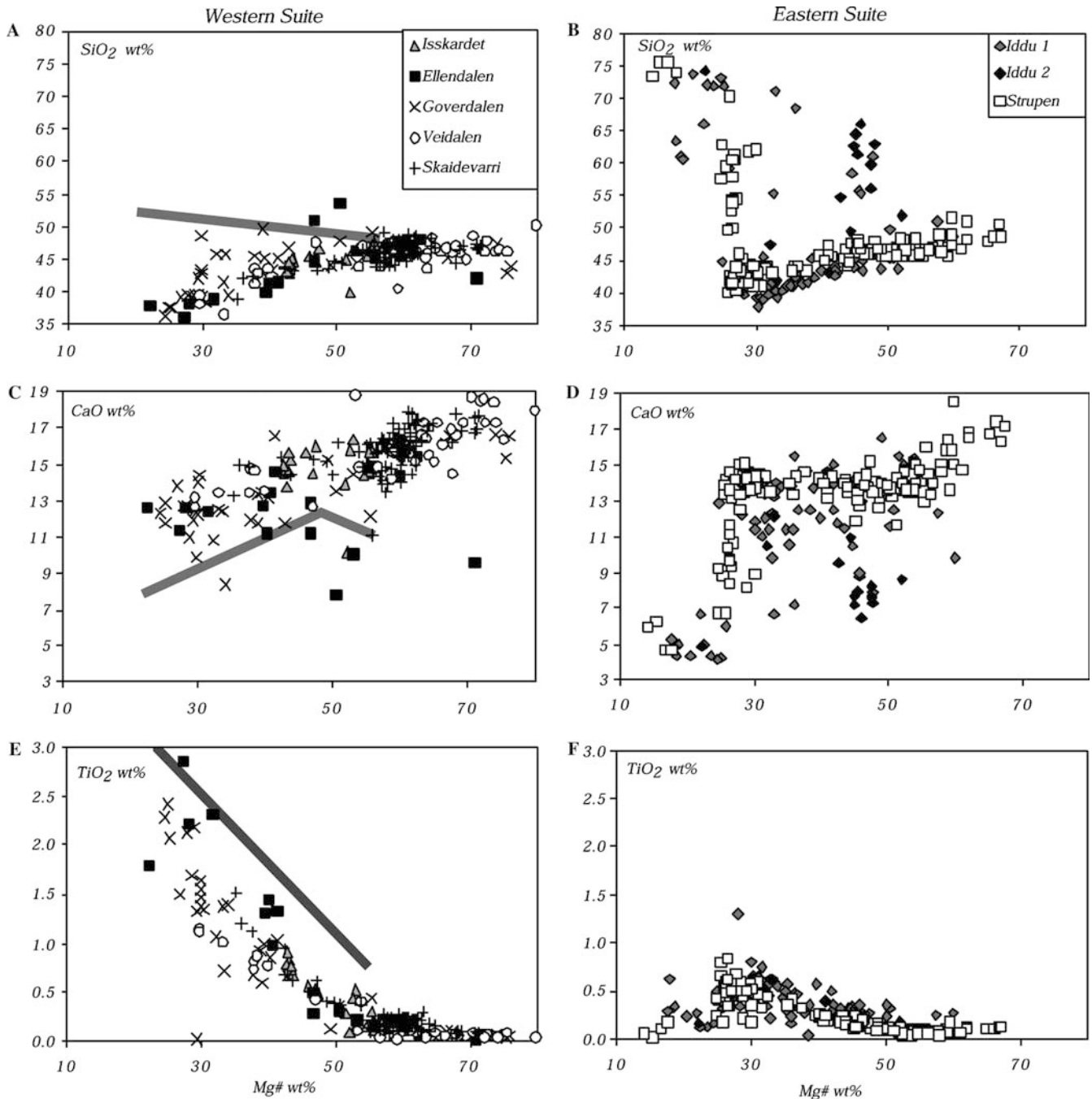


Fig. 3 Whole-rock Mg# ($100 \times \text{MgO}/(\text{MgO} + \text{FeO}^*)$) (FeO^* = all Fe as FeO) is plotted vs. SiO₂, CaO and TiO₂ for the Western (*left*) and Eastern (*right*) suite. Note how the SiO₂ content in the gabbros correlates with Mg# which is the opposite of that of basalts (*gray line*). In the Eastern suite, the fractionation of magnetite causes the SiO₂ to increase

rocks were analyzed on the CAMECA IMS 3f ion probe at Woods Hole Oceanographic Institution following the methods of Shimizu and Hart (1982). A primary beam of O-ions was focussed to $\sim 20 \mu\text{m}$ for REE (La, Ce, Nd, Sm, Eu, Dy, Er, Yb) and $\sim 10 \mu\text{m}$ for other trace elements (Ti, V, Cr, Sr, Y, Zr). Molecular interferences were eliminated by energy filtering and a secondary

voltage offset of -30 to -60 V for the REE and -90 V for the other trace elements. Uncertainties based on counting statistics were 5–10% (1σ) for REE and 1–5% (1σ) for the other trace elements. The data are presented in Table 5.

Mobility of elements

The rocks of the Lyngen Gabbro have been exposed to several metamorphic events, ranging from lower greenschist-facies to upper amphibolite- and possibly granulite-facies metamorphism. Several studies have investigated

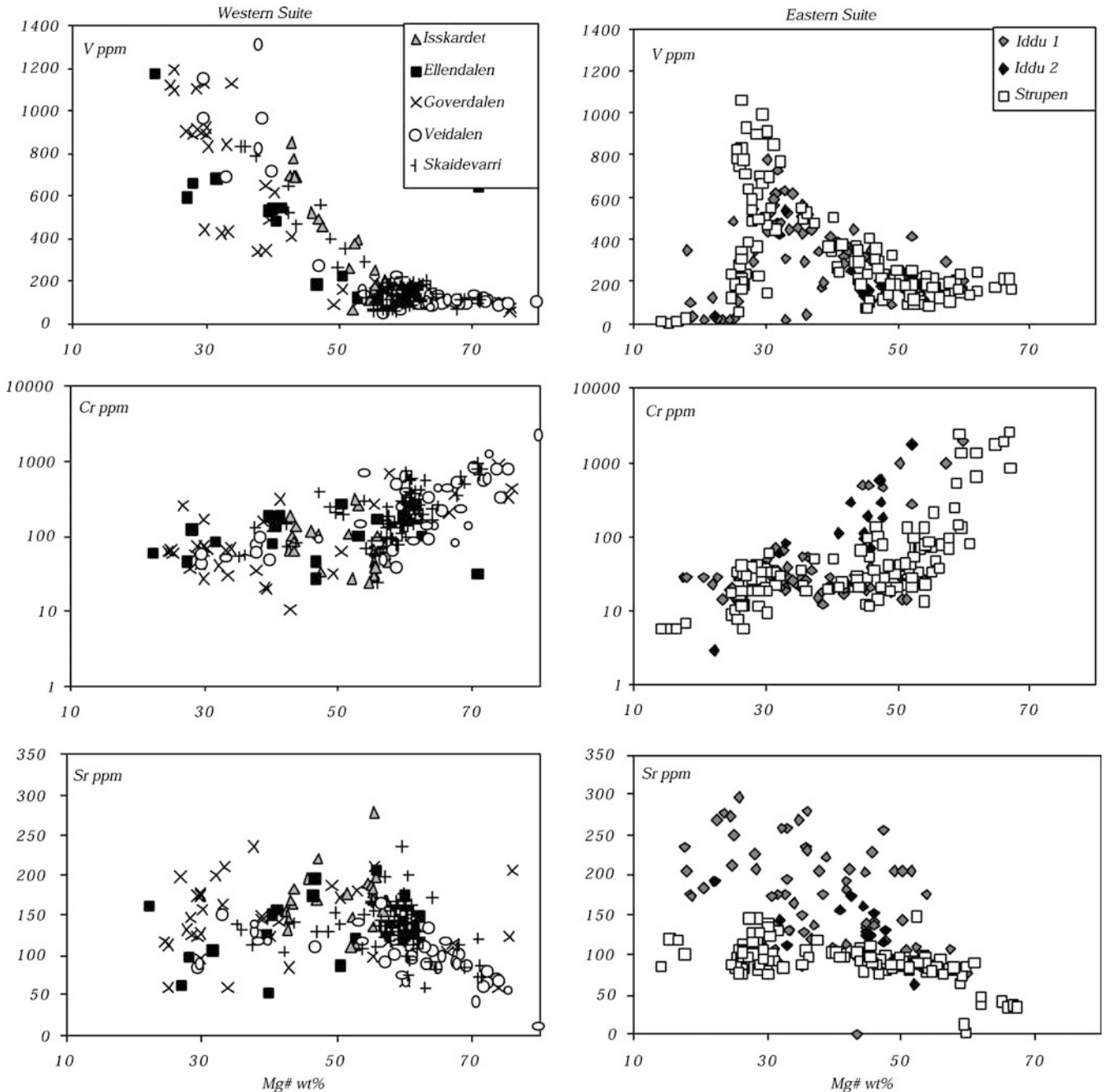


Fig. 4 Whole-rock Mg# (wt%) vs. trace elements for the Western (*left*) and Eastern (*right*) suite. See text for detailed descriptions

how elements are leached or enriched due to metamorphism of magmatic rocks. Cann (1970) and Coish (1977) investigated the mobility of different elements during sea-floor metamorphism, concluding that Ti, P, Y, Zr, Nb, Cr, and Ni are stable during greenschist-facies metamorphism. Shervais (1982) showed Ti and V to be stable under a wide range of metamorphic conditions, ranging from sea-floor metamorphism to granulite facies metamorphism. Elliot et al. (1997) investigated gabbros that occur as isolated masses within amphibolites, and

concluded that TiO_2 , FeO^t , MgO , MnO , and Na_2O and possibly Al_2O_3 were stable during amphibolite facies metamorphism. Weaver and Tarney (1981) analyzed mafic and ultramafic dikes cutting retrograded dikes, comparing dikes exposed to varying degree of metamorphism to fresh dikes. They concluded that Nd, P, Hf, Zr, Ti and the middle to heavy REE's are immobile even during strong metamorphism with access to fluids. An investigation of gneisses from a mylonitic shear zone shows that SiO_2 , K_2O , Na_2O , FeO^t and CaO are mobile when fluid phases are present (Sinha and Hewitt 1986).

In general, it is difficult to determine whether an element is mobile or not, and whether it will be enriched or depleted during alteration and metamorphism.

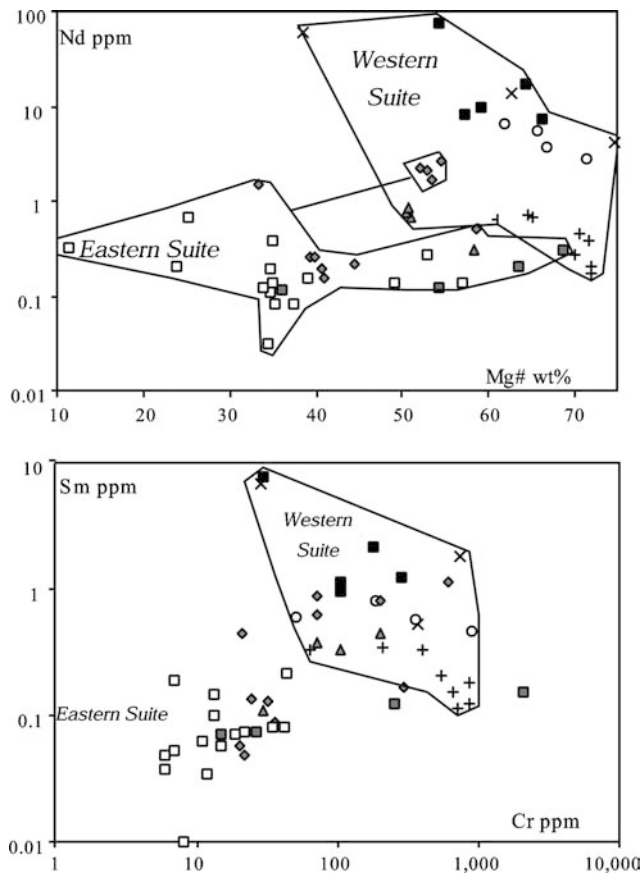


Fig. 5 Whole-rock analyses of the Lyngen Gabbro. Symbols are the same as for Fig. 4. The gray squares represent the lower 50 m from Strupen. Note the generally low contents of the incompatible trace elements in for the Eastern suite, whereas the Western suite has higher trace element concentrations that increase with differentiation

However, the above studies have shown that Zr, Y, P, Nb, Cr, Al, Ti, V and the REE will be relatively stable during the metamorphic conditions shown to be present along the composite cross-section. The ratios between these elements will hence be an accurate way to compare the rocks. MgO and FeO^l concentrations are also stable in the gabbros at higher metamorphic grades. As Sr is

unstable during alteration, no Sr isotopic analyses have been attempted.

Results

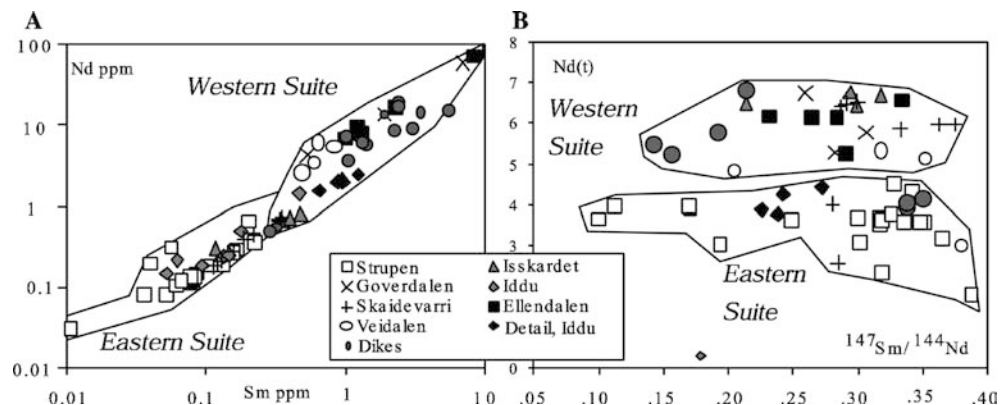
Whole-rock analyses of major elements

The whole-rock compositions of the gabbroic rocks largely reflect the minerals they are made up of. The gabbroic rocks from the Western suite of the Lyngen Gabbro are, in general, very low in silica (Fig. 2), few samples analyzed from the Western suite have higher than 50 wt% SiO₂, and the average is 45.5 wt%. However, the rocks are not ultramafic per se, but contains high-Ca plagioclase in the primitive cumulates, and increasing amounts of oxides as the rocks become more evolved. As the SiO₂ contents behave so differently between the suites, the degree of differentiation is explored using Mg#'s (100× MgO/(MgO + FeO)) in wt-%.) The trend of decreasing SiO₂ with increased differentiation is evident in the Western suite (Fig. 3a, b). Although the Eastern suite follows a similar trend for the majority of the samples, some show a clear Si-enrichment reflecting the high-Ca tonalites that were described by Hetland (1996) but less than 5% of the sampled rocks of the Eastern suite are such high-silica differentiates. Na₂O varies from traces to 4 wt%, but there is no clear correlation between SiO₂ and Na₂O in the Western suite, whereas the sodium-content increases with SiO₂ in the Eastern suite. K₂O and P₂O₅ are extremely low, and rarely exceed 0.1 wt%.

The CaO (Fig. 3c, d) contents decrease gradually during fractionation in the Western suite. However, the Eastern suite, and in particular the Strupen profile, shows near constant CaO-levels until the onset of SiO₂ enrichment.

The TiO₂ contents are dramatically different between the two suites (Figs. 2e, f and 3e, f). The Eastern suite shows few rocks with TiO₂ higher than 1 wt%, whereas the Western suite has up to 3 wt% in the most SiO₂-poor rocks, due to a higher percentage of ilmenite in the oxide-minerals. At around Mg# 30, the TiO₂ levels drop off for the Eastern suite, whereas they increase steeply for the Western suite. Thus, the in cumulates of the

Fig. 6 Sm-Nd element and isotope analyses of the Lyngen Gabbro and associated dikes. **a** The correlation between Sm and Nd concentrations in the Western and Eastern suite. **b** The $\epsilon_{Nd}(t=480 \text{ My})$ values generally fall in two groups, and the mafic dikes are present in both



Eastern suite, the evolved iron-rich melts precipitated iron–titanium oxides within the cumulate pile and expelled the evolved melts, producing the subsequent tonalitic rocks within the layered series.

Trace elements

The trace elements partly reflect what is observed in the major elements. It should be noted that many of the incompatible elements like Zr and Y are very close to the detection level of the XRF-method, especially in the Eastern suite.

Figure 4 demonstrates vanadium levels with similar trends as TiO_2 in Fig. 3. V behaves similarly to TiO_2 in these magmatic systems; e.g. relatively incompatible to silicate-minerals, but very compatible to magnetite and ilmenite (Shervais 1982). The matching V-contents of the Eastern and Western suite thus indicate the presence of oxide-minerals. The V contents do, however, decrease suddenly at lower Mg#’s for the Eastern suite, possibly indicating melt-mineral segregation leaving oxide-minerals in the cumulate. In addition, the Cr concentrations are similar between the two suites but become much lower relative to the Mg#’s in the Eastern suite than in the Western suite. The Sr contents show little in terms of systematic variations for either suite, but the concentrations are highest for the profile at Iddu.

Sm and Nd contents were measured by isotope dilution (Figs. 5 and 6a). These trace elements are highest in the Western suite, where they show some correlation with Cr or Mg#. The Eastern suite has concentrations below 1 ppm, and shows little correlation with either Cr or Mg#.

Nd-isotopes

The $\epsilon_{\text{Nd}(t=480\text{My})}$ values for the profiles are shown in Fig. 6b. The profiles from Ellendalen, Isskardet, and Goverdalen have the highest values, around +6. The Strupen samples and samples from the detailed profile at Iddu fall around +4. Veidalen samples fall in-between, whereas the Skaidevarri-profile shows values from both groups. The dikes that cross both suites and Rypdalen Shear Zone have ϵ_{Nd} values similar to the Western and Eastern suite.

Mineral analyses: major elements

The mineral compositions of plagioclase, augite, orthopyroxene and olivine and their range within each suite are listed in Table 4. There are distinct variations between the suites. Strupen, of the Eastern suite, has plagioclase An_{90-98} coexisting with Mg# 82-69 augite and Mg# 56-73 orthopyroxene. The upper half of the profile have the highest An contents of plagioclase found in the entire Lyngen Gabbro, and the lowest Mg#’s of clinopyroxene from this site. The lower half of the profile has

clinopyroxene with Mg#’s as high as 82 with plagioclase above An_{90} .

The profiles in Veidalen show similar plagioclase An-contents to those of Strupen, but coexisting with higher Mg# augite (88 to 72). This profile is also associated with the aforementioned layered peridotites, which have augite Mg#’s up to 92 and Fo_{88} olivine. West of this geochemical transition-zone, Goverdalen gabbros have An_{87-48} plagioclase, while their augites co-vary from Mg# 84 to 67.

The rocks of the Skaidevarre area have some plagioclase as high as An_{96} , although the majority of the plagioclases are approximately An_{85} , coexisting with Mg# 86-75 augite, Mg# 68-79 orthopyroxene and Fo_{66-78} olivine. The Easternmost rocks are the most primitive cumulates, and have plagioclase $\text{An}_{>90}$, where the mafic minerals become more evolved westwards. The Isskardet rocks have cumulates that are similar to Goverdalen and the evolved part of the Skaidevarre profile.

The rocks from Iddu vary greatly with regards to the plagioclase compositions (An_{56-75}) with a near constant composition of augite and orthopyroxene, and have no olivine together with plagioclase. It should be noted that many of these rocks are evolved quartz-bearing gabbros (see Table 2, series PA and PB).

Mineral analyses: trace elements

The rare-earth elements (REE) compositions of cores and rims of high-Ca pyroxenes from three of the areas; Goverdalen, Veidalen and Strupen, are shown in Fig. 7 and in Table 5. The samples were selected so that the most primitive and evolved sample, and an intermediate composition were analyzed. From Strupen, however, lithology types 1–4 were analyzed (type 5 does not contain augite). Reverse and normal zoning between the cores and rims are common in all the areas. The Goverdalen augites clearly have the highest concentrations of incompatible elements and the lowest of the compatible elements. La ranges from 0.6 to 0.12 ppm, and Cr from ~70 to ~500 ppm. Veidalen is intermediate, La varies from 0.39 to 0.02 ppm and Cr from 151 to ~2,000 ppm. The rocks from Strupen, however, are different. The LREE are nearly constant, La varies from 0.03 to 0.07 ppm, whereas the HREE varies oppositely, from 1.15 to 0.32 ppm, causing crossing REE-patterns. The most refractory augite, of sample Lan38, contains almost 2,500 ppm Cr, while the rest of the lithologies have low concentrations, ≤ 90 ppm.

Discussion

Our results show that the Western suite generally is less silicic, has higher ϵ_{Nd} values and lower An-plagioclase than the Eastern suite. In addition, the Rypdalen Shear Zone is bifurcated in the south. It is necessary to explore how co-existing solid-solution minerals and trace-ele-

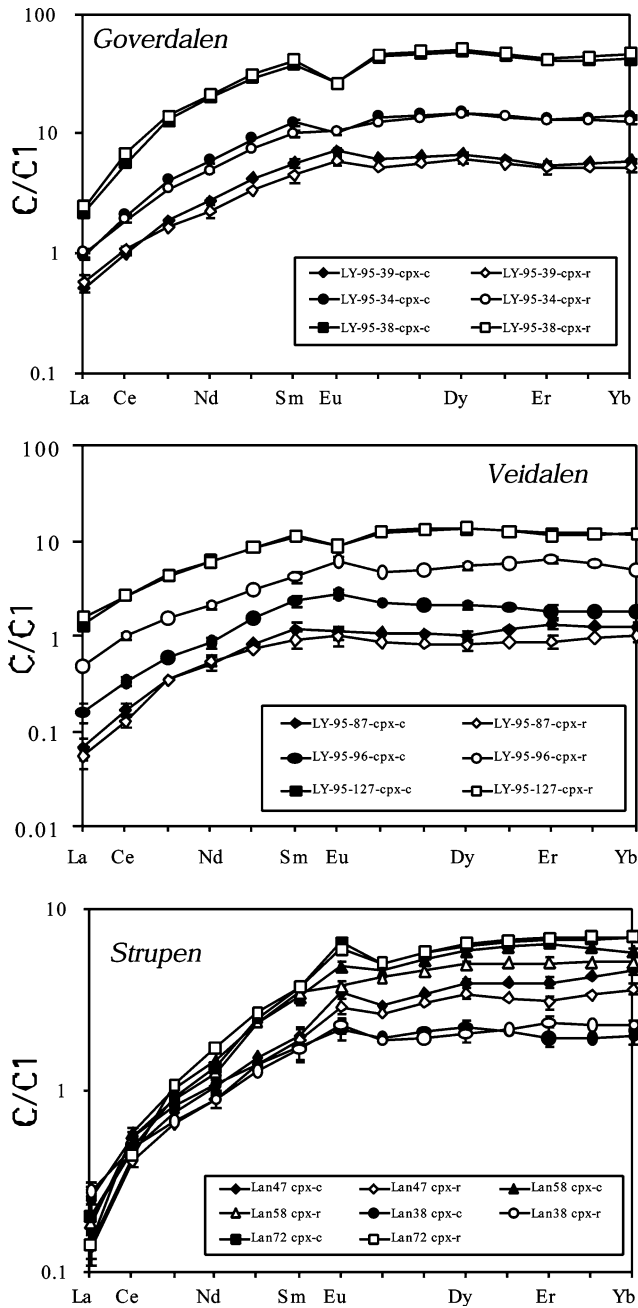


Fig. 7 REE patterns of gabbroic augite cores (filled symbols) and rims (open symbols) Strupen, Goverdalen and Veidalen. The REE data are normalized with relative abundances of C1 chondrite (Anders and Grevesse 1989)

ment mineral-compositions may be used to recognize under which magmatic conditions the cumulates and thus the dismembered ophiolite formed.

Parental magma compositions

The clinopyroxene mineral compositions reflect the trace-element compositions of the melt that produced them. We used the most primitive augite-cores analyses

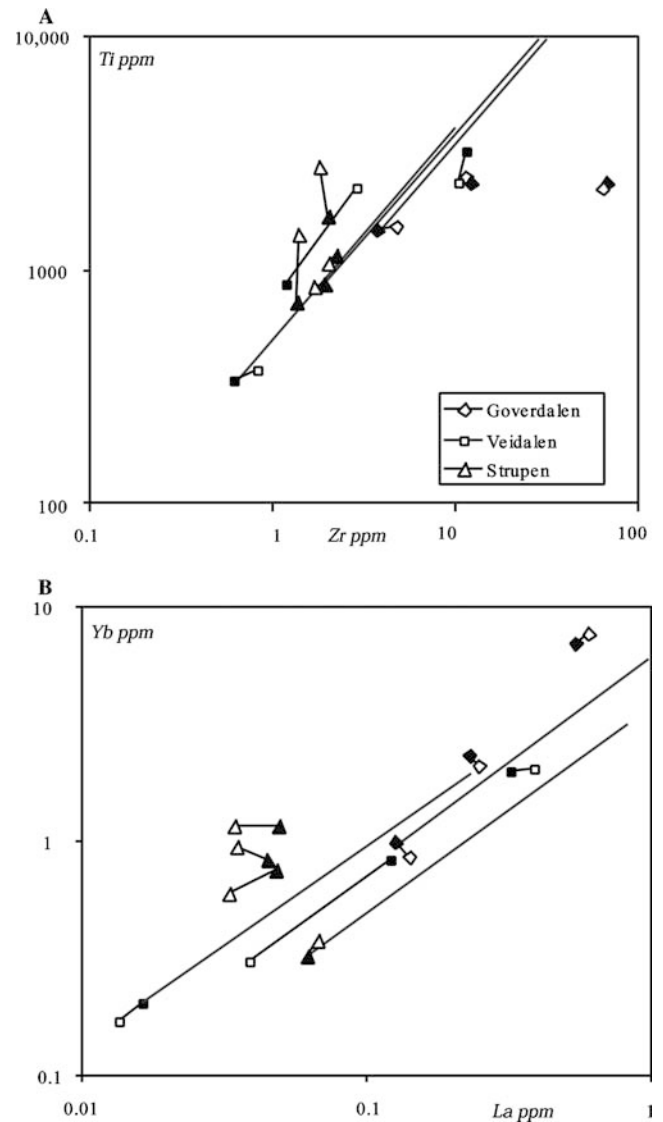


Fig. 8 Trace element data for clinopyroxene as measured in situ by the ion-probe. The cores (filled symbols) and rims (open symbols) of individual crystals are connected with a line. The gray lines represent solid-lines of descent for 90% fractional crystallization of 60% plagioclase and 40% augite. $Kd^{cpx/L}_{Ti}=0.4$, $Kd^{cpx/L}_{Zr}=0.1$, $Kd^{cpx/L}_{La}=0.056$, $Kd^{cpx/L}_{Yb}=0.0542$; $Kd^{pl/L}_{Ti}=0.04$, $Kd^{pl/L}_{Zr}=0.048$, $Kd^{pl/L}_{La}=0.19$, $Kd^{pl/L}_{Yb}=0.056$ (Arth 1976). See text for detailed description

from each area to calculate melt starting-compositions (Fig. 8). All these samples are gabbros, and we use a simple fractional crystallization model with 60% plagioclase and 40% clinopyroxene to model the evolution. However, the model describes neither of the magmatic series exactly. Goverdalen and Veidalen come close, reflecting near 90% fractionation between the most primitive and evolved rock (Fig. 7). Their oxide-gabbros augites clearly have lost Ti relative to Zr, which was to be expected. However, the partition-coefficients for the REE in ilmenite are very low and alike for La and Yb (Green 1994). The rocks from Goverdalen become slightly more LREE/HREE depleted with fractionation,

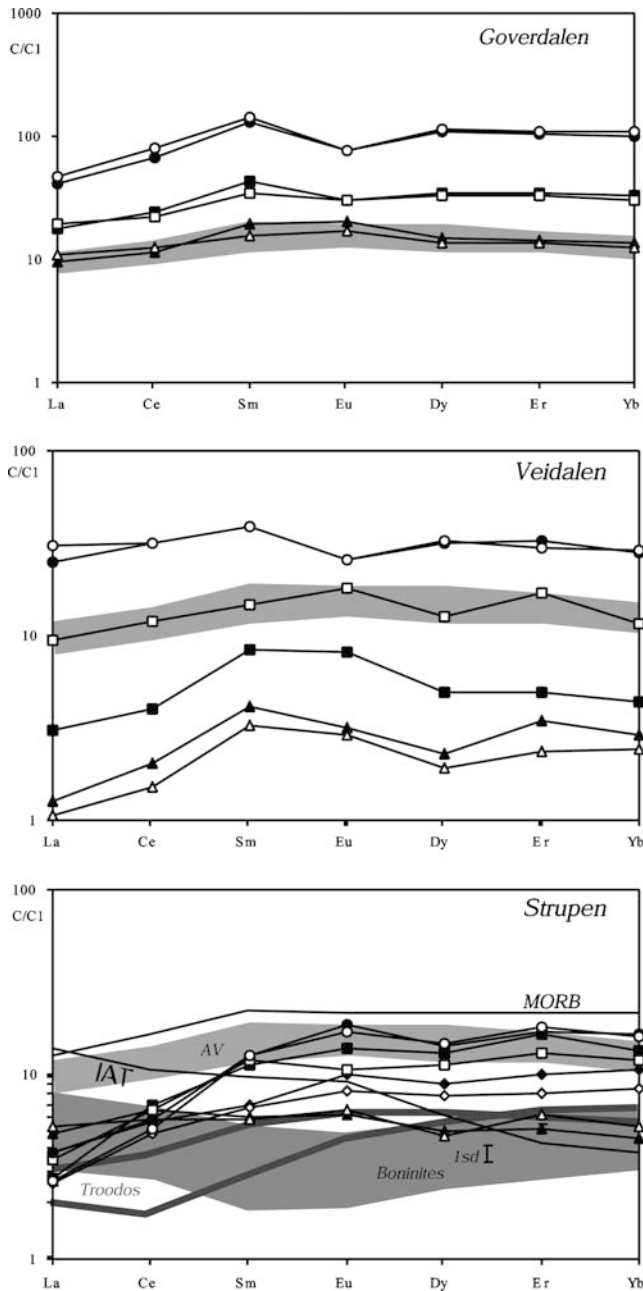


Fig. 9 Each of the trace element mineral analyses has been recalculated to melt-compositions by using K_d 's for clinopyroxene (Arth 1976). The compositions of MORB, IAT (Pearce 1983), Aksla Volcanics (Kvassnes 1997), boninites (Walker and Cameron 1980) and high-Ca Troodos lavas (Kostopoulos and Murton 1992) are compared to Strupen, Veidalen and Goverdalen. See text for further explanation.

whereas the Veidalen lithologies becomes enriched with crystallization. The latter may be explained by in-situ crystallization (Langmuir 1989) but the former cannot. Fractionation of more plagioclase relative to augite does reduce the La/Yb ratio slightly, however it also decreases the Zr/Ti ratio, which is not the case in the rocks. Including other minerals silicic minerals into the model will mostly change the degree of crystallization, not the

trend. The mineral-chemistry of the Strupen lithologies is very different from those from the other areas. Zr and La stays almost constant, whereas Ti and Yb increase with fractionation. No crystallization model can explain this trend, suggesting source-evolution or crustal contamination (DePaolo 1981).

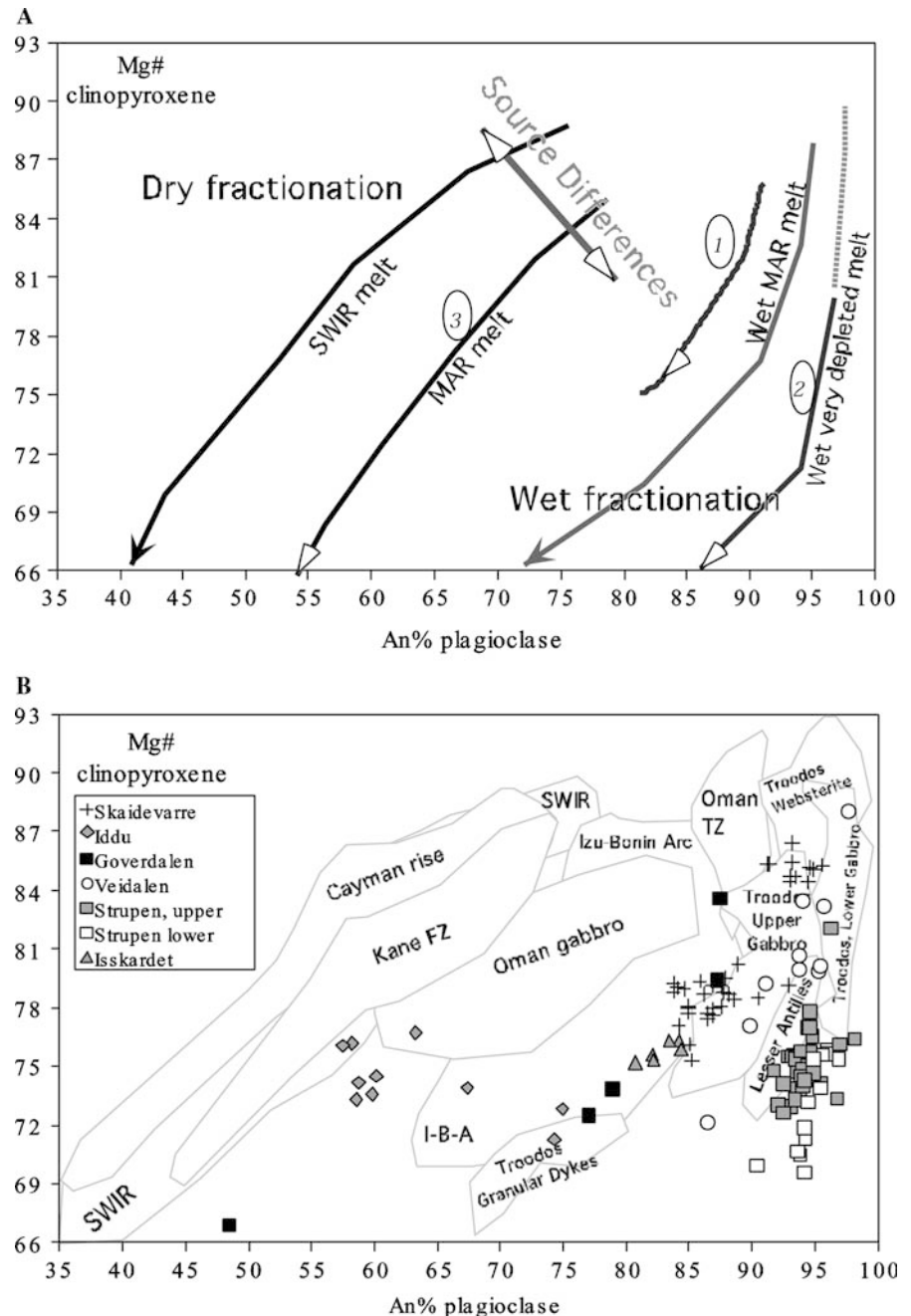
The calculated REE-melt compositions are compared to N-MORB, IAT (Sun 1980), the Aksla Volcanics (Furnes and Pedersen 1995), boninites (Hickey and Frey 1982) and Troodos lavas (Taylor and Nesbitt 1988) in Fig. 9. The result supports that Goverdalen gabbros and Veidalen gabbros may have crystallized from magma similar to the Aksla Volcanics or an N-MORB as their REE patterns are nearly parallel. The Strupen augites, however, crystallized from ultra-depleted magmas not enriched in LREE, similar to some high-Ca boninitic lavas from Troodos, different from the low-Ca boninitic lavas from Troodos that have LREE enrichment and a U-shaped pattern (Taylor and Nesbitt 1988).

Solid lines of descent for the Eastern and Western suites

Boninites are believed derived from wet melting of peridotitic sources after MORB extraction and water-extraction from the subducting plate (Crawford et al. 1989; Kelemen et al. 1997). It is difficult to determine whether the parental magmas were hydrous based on trace-elements or isotopes alone. Thus, we have explored the effect that water-activity and source-affinity of the magmas had on the petrogenesis of the Western and Eastern suite layered rocks, using the $An\%(pl)-Mg\#(cpx)$ plot. This diagram may distinguish the gabbroic rocks precipitated from a hydrous magma from a dryer one by the arc of the solid-line of descent (Fig. 10a). We assume that the mineral-compositions in each of the gabbros directly relates to the melt that precipitated them, and that the coexisting minerals precipitated from the same magma.

The presence of water suppresses the plagioclase-olivine cotectic relative to the plagioclase-augite cotectic (Gaetani et al. 1993) and changes the reaction series so augite or even orthopyroxene crystallize before plagioclase. In addition, a melt may gain or lose water so that $K_d^{Ca/Na}_{Pl/L}$ changes, resulting in higher or lower $An\%$ plagioclase, respectively (Housh and Luhr 1991). The effect is even more pronounced in magmas where quartz is crystallizing (Arculus and Wills 1990) and may cause $An_{>95}$ for more than 50% of the fractionating gabbros preceded by plagioclase-free cumulates. Early fractionation of clinopyroxene before plagioclase results in a significant drop in Mg-content in the magma at a more rapid rate than if plagioclase was crystallized in concert with olivine only. Moreover, prevalent water variably depresses the liquidii and solidii of the silicic minerals, whereas there is little effect on the oxide-minerals in magmas (Gaetani et al. 1993) and the bend of the gabbro-trend produced by wet magma fractionation is caused by the onset of oxide fractionation.

Fig. 10 a An content of plagioclase vs. Mg# (molar) of augite; MELTS models for dry and wet solid lines of descent of an enriched (SWIR) and a depleted (MAR) mid-ocean ridge melt, and dike 95LY71 (arrow 2). See text for detailed description. **b** An content of plagioclase vs. Mg# (molar) of augite for the Lyngen Gabbro compared to areas around the world. SWIR South West Indian Ridge (Dick et al. 2000), Cayman Rise (Elthon 1987), Kane FZ (Fracture Zone) (Cannat et al. 1997), Izu Bonin Arc (phenocrysts) (Sieger et al. 1992), Troodos data (Thy et al. 1989), Oman TZ (Maqsad area) Korenaga and Kelemen (1997), Oman gabbro (Kelemen et al. 1997), Hebert and Laurent 1990), Lesser Antilles (xenoliths) (Arculus and Wills 1990)



Dryer oceanic magmas, where plagioclase reaches the liquidus before clinopyroxene, experience a slower fractionation of Mg/Fe from the magma relative to Ca/Na in part because Ca is not depleted by augite-fractionation at an early stage. In addition, $Kd^{Ca/Na}_{PI/L} \approx 1$ (Grove et al. 1992), thus the An-content of a plagioclase reflects the Ca/Na-ratio of the parent-melt more directly. The vertical displacement of the curve varies with the Ca/Na and Mg/Fe of the melt (Fig. 10a). Thus, dry fractionation of basaltic melt produces a convex solid-line of descent whereas those for crystallization of wet melts are concave.

Increasing pressure lowers $Kd^{Ca/Na}_{PI/L}$ and leads to the formation of a lower An% plagioclase (Panjasa-

watwong et al. 1995). In addition, the pressure depresses the plagioclase-olivine cotectic relative to the olivine-clinopyroxene cotectic, and the Ca-Tschermak-component of the clinopyroxene increases (Gaetani et al. 1993). The result of fractionation at high pressures lead to ultramafic rocks with high-Al augite, followed by gabbroic cumulate with a convex trend, plagioclase starting at relatively low An-contents.

We used MELTS (Ghiorso and Sack 1995) to estimate the crystallization-conditions for our samples (arrows 1–3 in Fig. 10a). It has been argued that the MELTS program reproduces wet and intermediate pressures poorly (Yang et al. 1996). However, the high $Kd^{Ca/Na}_{PI/L}$ values we find in our models are comparable

to those of hydrous melts (Housh and Luhr 1991), and the partition-coefficients for the mafic minerals are reasonable. A primitive MAR melt extracted from PetDB was used as an initial composition and partly reproduced fractionation-trends for Goverdalen and Skaidivarri by adding up to 2 wt% water to the melt at low crustal pressures (1 kbar) (arrow 1), similar to the Upper Gabbro from Troodos (Fig. 10b). Plagioclase-free wehrlites are common in the Western suite (Kvassnes 1997), and cumulative, plagioclase-free harzburgites and lherzolites are found in the Eastern suite (Hetland 1996). Addition of water to MAR-type melts or crystallization at higher pressures cannot reproduce the Strupen trend alone, as the Ca/Na of the melt is too low. The Eastern suite gabbros have mineral-compositions similar to the Lower Gabbros from Troodos (Fig. 10b) and the Lesser Antilles lower-crustal xenoliths, which Arculus and Wills (1990) demonstrated crystallized under hydrous conditions in a silicic magma. Water-saturated crystallization of a dike ($\epsilon_{\text{Nd}(t=480\text{My})}$ of 4.1) that cross-cuts the Western suite in Goverdalen (sample 95LY71 as shown by arrow 2 in Fig. 10a) reproduces the solid-line of descent well. The difference between the upper and lower half of the Strupen profile can be explained by the addition of just a little more water to the magma that produced the upper half.

Dry fractionation (arrow 3) may replicate some of the gabbros at Iddu. The Iddu gabbro-compositions, however, do not have a clear solid-line of descent, ranging from the field of the Izu-Bonin Arc to the Mid-Atlantic Ridge (Kane FZ). The rocks are nothing like the active mid-ocean ridges, shown by the convex trend of the Mid-Cayman Rise gabbro and the South West Indian Ridge, and MAR gabbros, where the Ca/Na of the melt is lower and Mg/Fe is higher (Fig. 10b). Some of the analyzed rocks at Iddu have quartz as an essential mineral, and the high Si content of the magma may have influenced the plagioclase Ca/Na ratio and thus the solid-line of descent.

Temporal and spatial relations between the Western and Eastern suite

The gabbros in the Eastern suite uniformly have lower ϵ_{Nd} values than the Western suite and each suite follow separate, but parallel isochrons (not shown), suggesting similar ages of the suites. The oceanic Rypdalen Shear Zone generally separates the two suites in the northern half of the Lyngen Peninsula. In Skaidivarri, however, we sampled a section of layered and massive gabbros that changes from eastern suite signatures directly into western suite signatures over less than 10 m. The observation is supported both by the ϵ_{Nd} values (Fig. 6), and by the coexisting plagioclase and clinopyroxene compositions (Fig. 10b). Since the most primitive rocks are those with low ϵ_{Nd} it is not likely that the magma was contaminated by assimilation within the magma-chamber, thus the Skaidivarri-profile was sampled

across a magmatic transition between the two suites. The layered series has no later intrusive or tectonic contacts, indicating that the two magmatic systems coexisted, while the gabbros are cut by the Rypdalen Shear Zone further to the west than the contact between the suites. In the south, the Rypdalen Shear Zone appears twice, both in Goverdalen and Veidalen. It is therefore unlikely that the large shear zone caused the boninitic cumulates to be emplaced together with the tholeiitic gabbros. Rather, we suggest that parts of the complex magmatism happened concurrently, and the rest of the Lyngen Magmatic Complex was produced with close proximity between the suites.

Palaeo-environment of the Lyngen Gabbro

Back-arc and fore-arc type magmatic rocks often occur together in ophiolites. For example, Schouten and Kelenen (2002) demonstrated that the lower (tholeiitic) and upper (boninitic) lavas in the Troodos Ophiolite are related to the Upper and Lower Gabbros, respectively, and they argue that the systems were contemporaneous. Taylor and Nesbitt (1988) showed REE-patterns that cross for the Troodos Upper Lavas, and Cameron (1993) points out that the trace-element and isotope affinities between the Upper and Lower Lavas are so different that they must have had different magma sources.

As mentioned in the introduction, the Izu-Bonin arc and other present-day systems comprise an outer-arc high, a boninitic fore-arc, an arc section and an actively spreading back-arc basin (Crawford et al. 1981; Taylor et al. 1992). It is less common to find coexisting back-arc, arc, and fore-arc basin magmatism obducted together in the same ophiolite (Taylor et al. 1992). In fact, there is no typical silicic or calc-alkaline arc-magmatism in the Lyngen Magmatic Complex, though an arc-section is present in the similar-aged ophiolites in southern part of Norway (e. g. the Karmøy Ophiolite of Pedersen and Hertogen 1990). Taylor et al. (1992) suggested that the conditions that produce boninites and tholeiites together is currently not active in the oceans today. However, it is often suggested that coexisting tholeiitic and boninitic magmatism is the result of incipient arcs, and part of the early arc of the Izu-Bonin arc is currently the outer-arc high. ODP-site 458, situated on the outer-arc high between the Mariana trench and -ridge (Hickey-Vargas 1989) did indeed find contemporaneously emplaced back-arc basin tholeiites and high-Ca boninite lavas. They suggest that the boninite parent-magmas were generated by high degrees of melting of a moderately depleted lithosphere residual from generating Philippine-sea MORB, and that hydrous melting at greater depth, possibly within the asthenosphere, generated the tholeiites.

We envision that the close proximity to the trench make the incipient-arc crust more likely to be emplaced into the deeper levels of an orogenic belt, preserving them during erosion and orogenic collapse. The closure

of the large Iapetus Ocean may have caused several slivers of the supra-subduction zone to be obducted onto the active continental margin, preserving only the incipient arc, the Lyngen Magmatic Complex, in this part of the Scandinavian Caledonides.

Conclusion

The Lyngen Gabbro comprises two magmatic suites of distinct magmatic characteristics. The Western suite precipitated from magma that could have been derived from the same system as the associated tholeiitic Aksla Volcanics and Kjosens Greenschist. The elevated An-content of the plagioclases relative to the mafic minerals, together with relatively high $\epsilon_{\text{Nd}(t)}$ values (+6), suggest hydrous tholeiites similar to those of back arc basins. The Eastern suite comprise cumulates that were crystallized from magmas similar to those of the ultra-depleted high-Ca boninitic magmas of fore-arcs. Extremely high-An plagioclases coexist with evolved mafic minerals and oxides, and the $\epsilon_{\text{Nd}(t)}$ values are lower (+4) than in the Western suite. No volcanic counterpart to the Eastern suite has been found, although dikes crosscutting the gabbros may represent the magma that formed them. The oceanic Rypdalen Shear Zone generally separates the two suites, but non-tectonic transitions from boninitic to island-arc tholeiitic affinities suggest the magmatism happened concurrently. The magmatic proximity between the suites and the absence of a regular arc section, suggest that the Lyngen Gabbro represents the lower crustal section of an incipient arc or outer-arc high of an Ordovician oceanic *supra-subduction* zone.

Acknowledgements The authors wish to thank Harald Furnes, Dagfinn Slagstad and Rune Selbekk for assistance in the field, and Ole Tumyr for assistance in the lab. This manuscript was improved by an early review by Rhea Workman and formal reviews by Don Elthon and Alan Boudreau. The study was supported by the Norwegian Research Council and is Woods Hole Oceanographic Institution contribution# 11229.

References

- Anders E, Grevesse N (1989) Abundances of the elements; meteoritic and solar. *Geochem Cosm Acta* 53(1):197–214
- Andresen A, Stelthenpohl MG (1994) Evidence of ophiolite obduction, terrain accretion and polyorogenic evolution of the north Scandinavian Caledonides. *Tectonophysics* 231:59–70
- Arculus RJ, Wills KJA (1990) The petrology of the plutonic rocks and inclusions from the Lesser Antilles Island Arc. *J Petrol* 21:743–799
- Arth JG (1976) Behaviour of trace elements during magmatic processes—a summary of theoretical models and their applications. *J Res US Geol Surv* 4:41–47
- Cameron WE (1993) Petrology and origin of primitive lavas from the Troodos ophiolite, Cyprus. *Contrib Mineral Petrol* 89(2–3):239–255
- Cann JR (1970) Rb, Sr, Y, Zr and Nb in some Ocean Floor Basaltic Rocks. *Earth Planet Sci Lett* 10:7–11
- Cannat M, Chatin F, Whitechurch H, Ceuleneer G (1997) Gabbroic rocks trapped in the upper mantle in the Mid-Atlantic Ridge. In: Karson JA, Cannat M, Miller DJ, Agar SM, Barling J, Casey JF, Ceuleneer G, Dilek Y, Fletcher JM, Fujibayashi N, Gaggero L, Gee JS, Hurst SD, Kelley DS, Kempton PD, Lawrence RM, Marchig V, Mutter C, Niida K, Rodway K, Ross DK, Stephens CJ, Werner C-D, Whitechurch H, Stokking L (eds) *Proceedings of the ocean drilling program, scientific results* 153:243–264
- Chroston PN (1972) A gravity profile across Lyngnehalvøya, Troms, Northern Norway. *Norsk Geologisk Tidsskrift* 55:295–303
- Coish RA (1977) Ocean-floor metamorphism in the Betts cove Ophiolite, Newfoundland. *Contrib Mineral Petrol* 60:255–270
- Crawford AJ, Beccaluva L, Serri G (1981) Tectonomagmatic evolution of the West Philippine-Mariana region and the origin of boninites. *Earth Planet Sci Lett* 54:346–356
- Crawford AJ, Falloon TJ, Green DH (1989) Classification, petrogenesis and tectonic setting of boninites. In: Crawford AJ (ed) *Boninites and related rocks*. Allen & Unwin, New Zealand, pp 2–49
- Dallmeyer RD, Andresen A (1992) Polyphase tectonothermal evolution of exotic Caledonian nappes in Troms, Norway; evidence from $^{40}\text{Ar}/^{39}\text{Ar}$ mineral ages. *Lithos* 29(1–2):19–42
- DePaolo DJ (1981) Trace element and isotopic effects of combined wallrock assimilation and fractional crystallization. *Earth Planet Sci Lett* 53 (2):189–202
- Dick HJB, Natland JH, Alt JC, Bach W, Bideau D, Gee JS, Haggas S, Hertogen JGH, Hirth JG, Holm PM, Ildefonse B, Iturrino GJ, John BE, Kelley DS, Kikawa E, Kingdon A, LeRoux PJ, Maeda J, Meyer PS, Miller DJ, Naslund HR, Niu YL, Robinson PT, Snow J, Stephen RA, Trimby PW, Worm HU, Yoshinobu A (2000) A long in situ section of the lower ocean crust; results of ODP Leg 176 drilling at the Southwest Indian Ridge. *Earth Planet Sci Lett* 179(1):31–51
- Dunning GR, Pedersen RB (1988) U/Pb ages of ophiolites and arc-related plutons of the Norwegian Caledonides: implications for the development of Iapetus. *Contrib Mineral Petrol* 98:13–23
- Elliot T, Plank T, Morris J, Zindler A (1997) Timescales and element transport in the subduction zone: the Mariana arc as a representative case study. In: *Abstract of rates and timescales of magmatic processes*. Geol. Soc. Lon, London
- Elthon D (1987) Petrology of gabbroic rocks from the Mid-Cayman Rise spreading center. *J Geophys Res* 92(B1):658–682
- Elthon D, Stewart M, Ross DK (1994) Compositional trends of minerals in oceanic cumulates. *J Geophys Res* 97(B11):15189–15192
- Emeleus GH, Cheadle MJ, Hunter RH, Upton BGC, Wadsworth WJ (1996) The Rum Layered suite. In: Cawthorn RG (ed) *Layered intrusions*. Elsevier, Amsterdam
- Furnes H, Pedersen RB (1995) The Lyngen magmatic complex: geology and geochemistry *Geonytt* 22:30
- Gaetani GA, Grove TL, Bryan WB (1993) The influence of water on the petrogenesis of subduction-related igneous rocks. *Nature* 365(6444):332–334
- Ghiorso MS, Sack RO (1995) Chemical mass transfer in magmatic processes, IV. A Revised and internally consistent thermodynamic model for the interpolation of liquid–solid equilibria in magmatic systems at elevated temperatures and pressures. *Contrib Mineral Petrol* 119:197–212
- Govindaraju K (1994) 1994 compilation of working values and sample description for 383 geostandards. *Geostand Newslett* 18 (special issue)
- Green TH (1994) Experimental studies of trace-element partitioning applicable to igneous petrogenesis—Sedona 16 years later. *Chem Geol* 117:1–36
- Grove TL, Kinzler RJ, Bryan WB (1992) Fractionation of Mid-Ocean Basalt (MORB). In: Morgan JP, Blackman DK, Sinton JM (eds) *Mantle flow and mid ocean ridges*. *Geophys Monogr* 71:281–310

- Hebert R, Laurent R (1990) Mineral chemistry of the plutonic section of the Troodos Ophiolite; new constraints for genesis of arc-related ophiolites. In: Ophiolites; oceanic analogues; proceedings of the symposium "Troodos 1987". Minist Agric and Nat Resour, Nicosia, Cyprus, pp 149–163
- Hetland A (1996) Petrology and petrogenesis of high-Ca tonalites and quartz-bearing gabbros within the layered series of Lyngen Magmatic Complex (Troms, Norway). Thesis for the Cand. Scient. Degree, University of Bergen
- Hickey RL, Frey FA (1982) Geochemical characteristics of boninite series volcanics: implications for their source. *Geochim Cosmochim Acta* 46:2099–2115
- Hickey-Vargas R (1989) Boninites and tholeiites from DSDP Site 458, Mariana Forearc. In: Crawford AJ (ed) Boninites. Unwin Hyman, London, pp 340–354
- Housh TB, Luhr JF (1991) Plagioclase-melt equilibria in hydrous systems. *Am Min* 76:477–492
- Jenner GA, Longerich HP, Jackson SE, Fryer BJ (1990) ICP-MS: a powerful new tool for high-precision trace elements analysis in earth sciences: evidence from analysis of selected USGS standards. *Chem Geol* 38:323–344
- Kelemen PB, Koga K, Shimizu N (1997) Geochemistry of gabbro sills in the crust-mantle transition zone of the Oman Ophiolite; implications for the origin of the oceanic crust. *Earth Planet Sci Lett* 146(3–4):475–488
- Korenaga J, Kelemen PB (1997) Origin of gabbro sills in the Moho transition zone of the Oman Ophiolite; implications for magma transport in the oceanic lower crust. *J Geophys Res* 102(B12):27729–27749
- Kostopoulos DK, Murton BJ (1992) Origin and distribution of components in boninite genesis: significance of the OIB component. In: Parson LM, Murton BJ, Browning P (eds) Ophiolites and their Modern Oceanic Analogues. *Geol Soc Special Publ* 60:133–154
- Kvassnes AJ (1997) The Western suite of the Lyngen Gabbro and its Petrogenetic relations to the Volcanic and Ultramafic rocks associated with the Lyngen Magmatic Complex in Troms, Northern Norway. Thesis for the Cand. Scient. Degree, University of Bergen
- Langmuir CH (1989) Geochemical consequences of in situ crystallization. *Nature* 340(6230):199–205
- Minsaas O (1981) Lyngenhavvøyas geologi, med spesiell vekt på den sedimentologiske utvikling av de ordovisisk-siluriske klastiske sekvenser som overligger Lyngen Gabbrokompleks, Troms. Cand. Scient. (The Geology of the Lyngen Peninsula, with special emphasis on the sedimentological development of the Ordovician-Silurian clastic sequences overlying Lyngen Gabbro-complex.) Thesis, University of Bergen
- Minsaas O, Sturt BA (1985) The Ordovician-Silurian clastics sequence overlying the Lyngen Gabbro Complex, and its environmental significance. In: Gee DG, Sturt BA (eds) The Caledonide Orogen: -Scandinavia and related areas, vol 1, pp 569–577
- Miyashiro A (1973) The Troodos Ophiolite Complex was probably formed in and Island Arc, *Earth Planet Sci Lett* 19:218–224
- Moen-Eikeland HE (1999) Intrusive relasjoner i og petrogense av gabbroiske og tonalittiske bergarter på Lyngstuva, Troms, nord Norge. (Intrusive relations in, and petrogenesis of gabbroic and tonalitic rocks at Lyngstuva, Troms, North Norway.) Thesis for the Cand. Scient Degree, University of Bergen
- Munday RJC (1974) The geology of the northern half of the Lyngen Peninsula, Troms, Norway. *Norsk Geologisk Tidsskrift* 54 (suppl 1):49–62
- Nicolas A (1989) Structures of ophiolites and dynamics of oceanic lithosphere. Kluwer, Dordrecht, p 367
- Oliver GH, Krogh TE (1995) U-Pb zircon ages of 469 ± 5 Ma for a metatonalite from the Kjosens Unit of the Lyngen magmatic complex, northern Norway. *Norges Geologiske Undersøkelser* 428:27–33
- Padfield T, Gray A (1971) Major element rock analyses by X-ray fluorescence: a simple fusion method. NV Philips, Eindhoven, Analytical Equipment FS 35
- Panjasawatwong Y, Danyushevsky LV, Crawford AJ, Harris KL (1995) An experimental study of the effects of melt composition on plagioclase; melt equilibria at 5 and 10 kbar; implications for the origin of magmatic high-An plagioclase. *Contrib Mineral Petrol* 118(4):420–432
- Pearce JA (1983) Role of the sub-continental lithosphere in magma genesis at active continental margins. In: Hawkesworth CJ, Norry MJ (eds) Continental basalts and mantle xenoliths. Shiva, Nantwich, pp 230–249
- Pedersen RB, Hertogen J (1990) Magmatic Evolution of the Karmøy Ophiolite Complex, SW Norway: relationships between MORB-IAT-boninitic-Calc-alkaline and alkaline magmatism. *Contrib Mineral Petrol* 104:227–293
- Pedersen RB, Furnes H (1991) Geology, magmatic affinity and geotectonic environment of some Caledonian ophiolites in Norway. *J Geodyn* 13:183–203
- Pin C, Briot D, Bassin C, Poitrasson F (1994) Concomitant separation of strontium and samarium neodymium for isotope analyses in silicate samples, based on extraction chromatography. *Anal Chim Acta* 298:209–217
- Randall BAO (1971) The igneous rocks of the Lyngen Peninsula, Troms, Norway. In: The Caledonian geology of northern Norway. *Bulletin—Norges Geologiske Undersøkelse* 269:143–146
- Richard P, Shimizu N, Allégre CJ (1976) $^{143}\text{Nd}/^{144}\text{Nd}$, a natural tracer: An application to oceanic basalts. *Earth Planet Sci Lett* 60:93–104
- Schouten H, Kelemen PB (2002) Melt viscosity, temperature and transport processes, Troodos Ophiolite, Cyprus. *Earth Planet Sci Lett* 201(2):337–352
- Selbekk RS (1995) Tonalitt genese i Lyngen Magmatiske kompleks, Troms. (Tonalite genesis in the Lyngen Magmatic Complex, Troms.) Thesis for the Cand. Scient. Degree, University of Bergen
- Selbekk RS, Furnes H, Pedersen RB, Skjerlie KP (1998) Contrasting tonalite genesis in the Lyngen magmatic complex, North Norwegian Caledonides. *Lithos* 42(3–4):241–268
- Selbekk RS, Bray CJ, Spooner ETC (2002) Formation of tonalite in island arcs by seawater-induced anatexis of mafic rocks; evidence from the Lyngen Magmatic Complex, North Norwegian Caledonides. *Chem Geol* 182:69–84
- Shervais JW (1982) Ti-V plots and the petrogenesis of modern and ophiolite lavas. *Earth Planet Sci Lett* 59:101–118
- Shimizu N, Hart SR (1982) Applications of the ion microprobe to geochemistry and cosmochemistry. *Annu Rev Earth Planet Sci* 10:483–526
- Sieger RvdL, Arculus RJ, Pearce JA, Murton BJ (1992) 10. Petrography, mineral chemistry and phase relations of the basement boninite series of site 786, Izu-Bonin forearc. In: Fryer P, Pearce JA, Stokking LB et al (eds) Proceedings of the ocean drilling program, College Station, 125:171–125
- Sinha AK, Hewitt DA (1986) Fluid interaction and element mobility in the development of ultramylonites. *Geology* 14:883–886
- Slagstad D (1995) Rypdalen skjærsone, en oceansk skjærsone i Lyngen Magmatiske Kompleks. (Rypdalen Shear Zone, an Oceanic Shearzone in the Lyngen magmatic complex.) Thesis for the Cand. Scient. Degree University of Bergen
- Sun S-S (1980) Lead isotopic study of young volcanic rocks from mid-ocean ridges, ocean islands and island arcs. *Philos Trans R Soc Lond A297*:409–445
- Taylor RN, Nesbitt RW (1988) Light rare-earth enrichment of supra subduction-zone mantle: evidence from the Troodos ophiolite, Cyprus. *Geology* 16:448–451
- Taylor RN, Bramley JM, Nesbitt RW (1992) Chemical transects across intra-oceanic arcs: implications for the tectonic setting of ophiolites. In: Parson LM, Murton BJ, Browning P (eds) Ophiolites and their Modern Oceanic Analogues. *Geol Soc Special Publ* 60:117–132

- Thy P, Schiffman P, Moores EM (1989) Igneous mineral stratigraphy and Chemistry of the Cyprus crustal study project drill core in the Plutonic sequences of the Troodos Ophiolite. In: Gibson IL, Malpas J, Robinson PT, Xenophontos C (eds) Cyprus crustal study project: initial report. Hole CY-4, pp 147–185
- Walker DA, Cameron WE (1980) Boninite primary magmas; evidence from the Cape Vogel Peninsula, PNG. *Contrib Mineral Petrol* 83(1–2):150–158
- Weaver BL, Tarney J (1981) Chemical changes during dyke metamorphism in high-grade basement terranes. *Nature* 289:47–49
- Yang HJ, Kinzler RJ, Grove TL (1996) Experiments and models of anhydrous, basaltic olivine-plagioclase-augite saturated melts from 0.001 to 10 kbar. *Contrib Mineral Petrol* 124(1):1–18